

AD-A072 358

MALLORY (P R) AND CO INC BURLINGTON MASS LAB FOR PH--ETC F/G 10/3
LITHIUM-THIONYL CHLORIDE BATTERY.(U)

JUL 79 A N DEY, W BOWDEN, J MILLER, P WITALIS DAAB07-78-C-0563

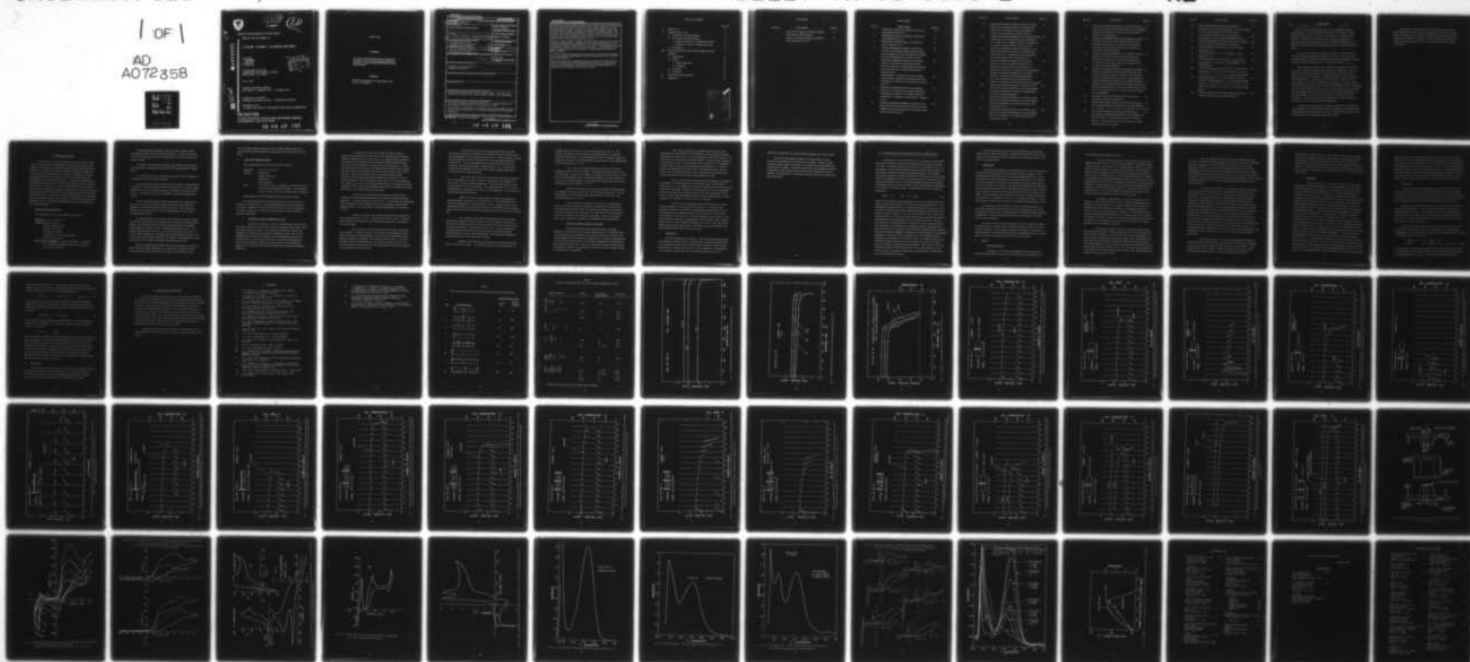
DELET-TR-78-0563-2

NL

UNCLASSIFIED

1 OF 1

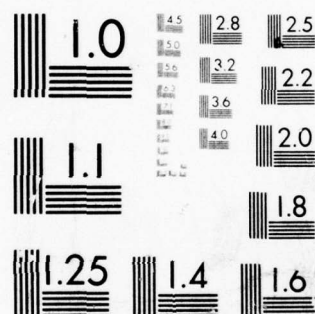
AD
A072358



END
DATE
FILMED

9-79

DDC



MICROCOPY RESOLUTION TEST CHART
NATIONAL BUREAU OF STANDARDS-1963-A



LEVEL III

A072358

A068422

12

Research and Development Technical Report

DELET-TR-78-0563-2

LITHIUM - THIONYL CHLORIDE BATTERY

A. N. DEY
W. BOWDEN
J. MILLER
P. WITALIS

P. R. MALLORY & CO. INC.
LABORATORY FOR PHYSICAL SCIENCE
BURLINGTON, MA 01803



JULY 1979

SECOND QUARTERLY REPORT
FOR PERIOD 1 JANUARY 1979 - 31 MARCH 1979

DISTRIBUTION STATEMENT :
APPROVED FOR PUBLIC RELEASE ; DISTRIBUTION UNLIMITED

PREPARED FOR :
US ARMY ELECTRONICS TECHNOLOGY AND DEVICES LABORATORY

ERADCOM

US ARMY ELECTRONICS RESEARCH AND DEVELOPMENT COMMAND
FORT MONMOUTH, NEW JERSEY 07703

79 08 03 131

A072358

DDC FILE COPY

NOTICES

Disclaimers

The citation of trade names and names of manufacturers in this report is not to be construed as official Government indorsement or approval of commercial products or services referenced herein.

Disposition

Destroy this report when it is no longer needed. Do not return it to the originator.

Unclassified

SECURITY CLASSIFICATION OF THIS PAGE (When Data Entered)

REPORT DOCUMENTATION PAGE		READ INSTRUCTIONS BEFORE COMPLETING FORM
1. REPORT NUMBER 18 DELET-TR-78-0563-2	2. GOVT ACCESSION NO.	3. RECIPIENT'S CATALOG NUMBER
4. TITLE (and Subtitle) 6 Lithium-Thionyl Chloride Battery	5. TYPE OF REPORT & PERIOD COVERED Second Quarterly 1/1/79 to 3/31/79	
		6. PERFORMING ORG. REPORT NUMBER
7. AUTHOR(s) 10 A. N. Dey, W. Bowden, J. Miller, P. Witalis	8. CONTRACT OR GRANT NUMBER(s) 15 DAAB07-78-C-0563	
9. PERFORMING ORGANIZATION NAME AND ADDRESS P. R. Mallory & Co. Inc. Laboratory for Physical Science Burlington, Mass. 01803	10. PROGRAM ELEMENT, PROJECT, TASK AREA & WORK UNIT NUMBERS 16 LL162705AH9411-219	
11. CONTROLLING OFFICE NAME AND ADDRESS U.S. Army Electronics Technology & Device Lab. ERADCOM Attn: DELET-PR Ft. Monmouth, New Jersey 07703	12. REPORT DATE 11 July 1979 17 11	
14. MONITORING AGENCY NAME & ADDRESS (if different from Controlling Office) 12 69 p. 1	13. NUMBER OF PAGES 55	
		15. SECURITY CLASS. (of this report) Unclassified
16. DISTRIBUTION STATEMENT (of this Report) Approved for Public Release Distribution Unlimited 9 Quarterly rept. no. 2, 1 Jan - 31 Mar 79		15a. DECLASSIFICATION/DOWNGRADING SCHEDULE
17. DISTRIBUTION STATEMENT (of the abstract entered in Block 20, if different from Report)		
18. SUPPLEMENTARY NOTES		
19. KEY WORDS (Continue on reverse side if necessary and identify by block number) Inorganic electrolyte battery, thionyl chloride, lithium, high rate D cell, high rate flat cylindrical cell, laser designator battery, cyclic voltammetry.		
20. ABSTRACT (Continue on reverse side if necessary and identify by block number) This report summarizes the activities carried out on Contract DAAB07-78-C-0563 during the period January 1, 1979 to March 31, 1979. The objectives of this program is to develop safe Li/SOCl ₂ batteries for high rate U.S. Army applications such as manpack radio (BA5590) and GLLD laser designators. During the first quarter we examined the effect of cathode current collector		

DD FORM 1 JAN 73 1473 EDITION OF 1 NOV 65 IS OBSOLETE

Unclassified

SECURITY CLASSIFICATION OF THIS PAGE (When Data Entered)

215 325 79 08 03 134

Unclassified

SECURITY CLASSIFICATION OF THIS PAGE(When Data Entered)

designs on the current carrying capability of the spirally wound D cells and the₂ flat cylindrical cells and found that short circuit current densities of 200mA/cm₂ may be realized by proper choice of the current collector design using a conventional cathode matrix. In addition we carried out a parallel research effort in order to gain increased understanding of the SOCl₂ reduction process. We showed, using cyclic voltammetry and coulometry, that the reduction of SOCl₂ does not lead to the immediate formation of S and SO₂ but to some other intermediates which slowly decompose to form SOCl₂.

During the second quarter, we tested high rate spirally wound D cells of various promising cathode designs on BA5590 and GLLD laser designator duty cycles. We found that Li/SOCl₂ BA5590 battery ran for 100 hrs at room temperature on the BA5590 duty cycle and weighed approximately 840 gm. This represents a 20% gain in service life and an 11% reduction in battery weight over that of the Li/SO₂ batteries.

Li/SOCl₂ D cells when tested on pro-rated bases on the GLLD laser designator duty cycle delivered approximately six times the service life of the presently used Ni/Cd batteries.

We have obtained some spectroscopic evidence in favor of the formation of at least two possible meta-stable intermediates resulting from the discharge of SOCl₂ at room temperature. These results have an important bearing on the devising of ways to improve the safety of the cells.

Unclassified

SECURITY CLASSIFICATION OF THIS PAGE(When Data Entered)

TABLE OF CONTENTS

	Page No.
I. Introduction	1
II. Spirally Wound D Cell	3
A. BA5590 Man Pack Radio Battery	3
B. GLLD Laser Designator Battery	5
1. Testing of D Cells vs. Modified Duty Cycle	5
2. Testing of D Cells vs. Regular Duty Cycle	8
C. Conclusions	9
III. Electrochemical and Spectroscopic Studies on SOCl_2 Reduction	11
A. Experimental	12
B. Results	12
1. Cyclic Voltammetry	12
2. Coulometry	15
C. Discussion	16
D. Conclusion	17
IV. Conclusions and Future Work	18
V. References	19

Accession For	
NTIS GRA&I	<input checked="checked" type="checkbox"/>
DDC TAB	<input type="checkbox"/>
Unannounced	<input type="checkbox"/>
Justification	
By	
Distribution/	
Availability Codes	
Dist	Avail and/or special
A	

List of Tables

Table No.	Table Caption	Page No.
1	Short-Circuit Currents of Hermetic D Cells with Various Cathode Designs	21
2	Behavior of High Rate Li/SOCl_2 D Cells on GLLD Modified Duty Cycle	22

List of Figures

Fig. No.	Figure Caption	Page No.
1.	Performance of high rate Li/SOCl_2 D cell on pro-rated BA5590 test at 25°C .	23
2.	Performance of high rate Li/SOCl_2 D cell on pro-rated BA5590 test at 0°C .	24
3.	Performance of BA5590 battery of 8 Li/SOCl_2 D cells in series at 25°C .	25
4.	Voltage and temperature profiles of Li/SOCl_2 D cell with 20 inch carbon cathode having a central tab on modified GLLD test consisting of 6.5A pulse of 3 minute duration every 27 minutes at 25°C .	26
5.	Voltage and temperature profiles of an insulated Li/SOCl_2 D cell with 20 inch carbon cathode having a central tab on modified GLLD test consisting of 8.0A pulse of 3 minute duration every 27 minutes at 25°C .	27
6.	Voltage profile of Li/SOCl_2 D cell with 20 inch cathode having a central tab on modified GLLD test consisting of a 3 minute 6.5A pulse every 27 minutes at -30°C .	28
7.	Voltage and temperature profiles of an insulated Li/SOCl_2 D cell with 20 inch cathode having both a horizontal and vertical tab on modified GLLD test consisting of a 3 minute 6.5A pulse every 27 minutes at 25°C .	29
8.	Voltage and temperature profiles of Li/SOCl_2 D cell with 25 inch cathode having one tab at one end on the modified GLLD test consisting of a 3 minute 8A pulse every 27 minutes at 25°C .	30

Fig. No.	Figure Caption	Page No.
9.	Voltage and temperature profiles of Li/SOCl_2 D cells having 25 inch cathode with both a horizontal and a vertical tab on modified GLLD test consisting of a 3 minute 6.5A pulse every 27 minutes at 25°C.	31
10.	Voltage and temperature profiles of an insulated Li/SOCl_2 D cell with 25 inch cathode having both a horizontal and a vertical tab on modified GLLD test consisting of a 3 minute 6.5A pulse every 27 minutes at 25°C.	32
11.	Voltage and temperature profiles of a Li/SOCl_2 D cell with 25 inch cathode having both a horizontal and a vertical tab on the modified GLLD test consisting of a 3 minute 8A pulse every 27 minutes at 25°C.	33
12.	Voltage and temperature profiles of an insulated Li/SOCl_2 D cell with 25 inch cathode having two tabs on the modified GLLD test consisting of a 3 minute 6.5A pulse every 27 minutes at room temperature.	34
13.	Voltage and temperature profiles of an insulated Li/SOCl_2 D cell with 25 inch cathode having two tabs on the modified GLLD test consisting of a 3 minute 8.0A pulse every 27 minutes at room temperature.	35
14.	Voltage and temperature profiles of a Li/SOCl_2 D cell with 25 inch cathode having three tabs on the modified GLLD test consisting of a 3 minute 6.5A pulse every 27 minutes at room temperature.	36
15.	Voltage and temperature profiles of a Li/SOCl_2 D cell with 25 inch cathode having three tabs on the modified GLLD test consisting of a 3 minute 6.5A pulse every 27 minutes at -30°C.	37
16.	Voltage and temperature profiles of a Li/SOCl_2 D cell with 25 inch cathode having three tabs on the modified GLLD test consisting of a 3 minute 6.5A pulse every 27 minutes at -30°C.	38

Fig. No.	Figure Caption	Page No.
17.	Voltage and temperature profiles of an insulated Li/SOCl ₂ D cell with 25 inch cathode having three tabs on the modified GLLD test consisting of a 3 minute 8.75A pulse every 27 minutes at room temperature.	39
18.	Voltage and temperature profiles of two parallel connected Li/SOCl ₂ D cells with 20 inch cathode having one tab located at the center on the actual GLLD test involving 17.5A and 1.8A consecutive pulses for 3 minutes every 27 minutes at room temperature.	40
19.	Voltage and temperature profiles of two parallel connected Li/SOCl ₂ D cells with 20 inch cathode having one tab located at the center on the actual GLLD test involving 17.5A and 1.8A consecutive pulses for 3 minutes every 27 minutes at room temperature.	41
20.	Voltage and temperature profiles of two parallel connected Li/SOCl ₂ D cells with 25 inch cathode having three tabs on actual GLLD test involving 17.5A and 1.8A consecutive pulses for 3 minutes every 27 minutes at room temperature.	42
21.	Voltage and temperature profiles of two parallel connected Li/SOCl ₂ D cells (with heat shrinkable jackets) with 25 inch cathode having three tabs on actual GLLD test involving 17.5A and 1.8A consecutive pulses for 3 minutes every 27 minutes at room temperature.	43
22.	Schematic drawing of the jacketed cell used for cyclic voltammetry at various temperatures.	44
23.	Cyclic voltammogram of SOCl ₂ in CH ₃ CN/0.1N N(C ₄ H ₉) ₄ PF ₆ showing the effect of sweep rate at a Pt wire electrode a) 0.20 V/sec b) 0.50 V/sec c) 1.0V/sec d) 2.0 V/sec	45
24.	Cyclic voltammograms of SOCl ₂ in CH ₃ CN/N(C ₄ H ₉) ₄ PF ₆ at various concentrations (upper) a) 25μl SOCl ₂ /75 ml (V=0.50 V/sec), b) 50μl SOCl ₂ /75 ml (V= 0.050 V/sec) (lower) c) 100μl SOCl ₂ /75 ml (V=0.20 V/sec), d) 200μl SOCl ₂ /75 ml (V= 0.20 V/sec).	46

Fig. No.	Figure Caption	Page No.
25.	Cyclic voltammograms of SOCl_2 in $\text{CH}_3\text{CN}/0.1\text{N}$ $\text{N}(\text{C}_4\text{H}_9)_4\text{PF}_6$ a) Ni wire electrode, b) Ir wire electrode, c) Au-Hg wire electrode ($V = .20\text{V}/\text{sec}$ in all).	47
26.	Cyclic voltammogram of SOCl_2 in $\text{CH}_3\text{CN}/0.1\text{N}$ $\text{N}(\text{C}_4\text{H}_9)_4\text{PF}_6$ at a silver wire electrode ($0.05\text{V}/\text{sec}$).	48
27.	Cyclic voltammogram of SOCl_2 in $\text{DMSO}/0.1\text{N}$ $\text{N}(\text{C}_4\text{H}_9)_4\text{PF}_6$ at a platinum wire electrode ($0.05\text{V}/\text{sec}$).	49
28.	UV-VIS spectrum of 2 mM SO_2 in CH_3CN vs CH_3CN (pathlength 1 cm).	50
29.	UV-VIS spectrum of $\sim 2\text{ mM}$ S in CH_3CN vs CH_3CN (pathlength 1 cm).	51
30.	UV-VIS spectrum of $\sim 1.8\text{ mM}$ SOCl_2 in $\text{CH}_3\text{CN}/0.1\text{N}$ $\text{N}(\text{C}_4\text{H}_9)_4\text{PF}_6$ vs $\text{CH}_3\text{CN}/0.1\text{N}$ $\text{N}(\text{C}_4\text{H}_9)_4\text{PF}_6$ in a 1 cm pathlength cell.	52
31.	Cyclic voltammogram of 1.8 mM SOCl_2 in $\text{CH}_3\text{CN}/0.1\text{N}$ $\text{N}(\text{C}_4\text{H}_9)_4\text{PF}_6$ a) $n = 0.00$, b) $n = 0.300$, c) $n = 0.84$, d) $n = 1.33$, e) $n = 1.76$, f) $n = 2.0$ after one week stand.	53
32.	Absorbance spectra of $\sim 1.8\text{ mM}$ solution of SOCl_2 in $\text{CH}_3\text{CN}/0.1\text{N}$ $\text{N}(\text{C}_4\text{H}_9)_4\text{PF}_6$: a) $n = 0.00$ (start of electrolysis), b) $n = 0.30$, c) $n = 0.84$, d) $n = 1.33$, e) $n = 1.33$ after 16 hour stand, f) $n = 1.76$, g) $n = 2.0$ after one week stand.	54
33.	Variation of λ_{max} and absorbance of SOCl_2 solution as a function of charge passed during electrolysis.	55

I. Introduction

↙ This report describes, # which
→ The Li/SOCl₂ inorganic electrolyte system (1-4) is the highest energy density system known to date. It consists of a Li anode, a carbon cathode and SOCl₂ which acts both as a solvent and as a cathode active material. The electrolyte salt that has been used most extensively is LiAlCl₄, but salts such as Li₂B₁₀Cl₁₀ (5) and Li₂O(AlCl₃)₂ (6) have also been used successfully in this system for improving the shelf life characteristics.

The main objective of this program is to develop high rate Li/SOCl₂ cells and batteries for portable applications of the U. S. Army. The cells and batteries must deliver higher energy densities than are presently available and must be safe to handle under U. S. Army field conditions. ↙

We carried out a detailed development (7) on the spirally-wound high rate D cells in order to establish their performance capabilities as well as to identify and correct the limitations in their performance and safety under various use and abuse conditions. Substantial progress was made to correct the cell limitations. We found that the state-of-the-art spirally-wound D cells approach the high rate requirements of the various U. S. Army applications more closely than do any other cell designs at the present time. Accordingly we have used this spirally-wound D cell as a starting point and have improved its rate capability to meet the requirements of two specific applications, viz. the BA5590 Battery for Man Pack Radio and the Battery for the GLLD Laser Designator. Our work during the second quarter was focussed primarily on the testing of D cells for the above two applications.

A parallel research effort was continued in order to gain an increased understanding of the cell discharge reactions, particularly with respect to the unstable intermediates. We believe that this knowledge will be useful in providing guidance for improving the safety of the system.

The progress in optimizing the high rate Li/SOCl_2 D cells for the BA5590 battery and the GLLD battery are described in this second quarterly report. In addition we have carried out electrochemical and spectroscopic experiments to clarify the mechanism of thionyl chloride reduction and subsequent chemical reactions in the cell. These results are also included in this report.

II. Spirally Wound D Cell

We found (21) that the current distribution of the high rate spirally wound D cells having one current collector tab located at one end of the cathode was controlled by the electrical conductivity of the cathode grid. Therefore, we examined the effect of a variety of cathode tab designs on the current carrying capability of the cathode as determined by the short circuit current density of the cathode. The results obtained during the preceding quarter are reproduced in Table 1. Note that by placing the tab in the middle as in design 2, the short circuit current density was increased from 53 mA/cm^2 to 168 mA/cm^2 . In view of the simplicity of this cathode design and the substantial improvement in performance, we chose this cathode design for the spirally wound D cells to be tested for BA5590 manpack radio battery application. In addition, we evaluated spirally wound D cells having the various cathode designs shown in Table 1 for the GLLD Laser Designator application as well. The experimental details and the results obtained to date are presented here.

A. BA5590 Manpack Radio Battery

The specifications of the above battery are as follows.

Dimension: 4.4" x 2.45" x 5.00"

Voltage: Nominal 12 or 24V

Maximum (OCV) 15 or 30V

Average 12.5 or 25V

End Voltage 10 or 20V

Capacity at 70°F 10 A.Hr (30 hr rate)

Max. Rate: 2 hr rate

Duty for 30 volt Operation: 8 Ω load for 100 msec followed by
39 Ω load for 1 min. followed by 560 Ω load for 9 min.

The above is repeated.

The presently used batteries contain 10 Li/SO_2 D cells in series and parallel to meet the 15 and 30 volt requirements. In view of the higher OCV of the Li/SOCl_2 D cells (3.6 volt) only eight D cells are needed for the required voltage.

We carried out the initial evaluations using single D cells instead of the 8 cell battery. Therefore, the duty cycle used was prorated for a single cell as:

1 Ω load for 100 msec followed by 5 Ω load for 1 min. followed by 70 Ω load for 9 min. The cycle is repeated.

One Li/SOCl_2 D cell with cathode having one tab in the middle (design 2 of Table 1) was tested under the above duty cycle at 25°C. The cell voltage under the 80 Ω and 5 Ω loads are plotted as a function of time and is shown in Fig. 1. The cell ran for 95 hours, delivering a capacity of approximately 10 A.Hr.

Another D cell with similar cathode was tested at 0°C under the same duty cycle. In this case the cell voltages under all the three loads were monitored as a function of time and are shown in Fig. 2. This cell ran for 93 hours to 2.5 volt cut off (on 1 Ω load) corresponding to a cell capacity of approximately 9.8 A.hr.

One BA5590 battery was assembled using 8 Li/SOCl_2 D cells in series. The battery was tested at room temperature on the battery duty cycle mentioned earlier. The battery voltage on the three loads and the battery temperature was monitored as a function of time. The results are shown in Fig. 3. The average battery voltages on the 8 Ω , 39 Ω and 560 Ω loads were 25.5, 27 and 28.5 volts respectively. The battery ran for approximately 100 hours to the 20 volt cutoff. The capacity delivered by the battery was approximately 11 A.Hr. The temperature of the battery remained unchanged during the test.

The above BA5590 battery weighed 840 gms and contained 8 D Li/SOCl_2 cells. The Li/SO_2 BA5590 batteries, on the other hand, contain 10 D cells and weigh 940 gms with a service life of 80 hours on the same duty cycle.

Thus, the improvement in performance of the Li/SOCl_2 BA5590 battery over that of the Li/SO_2 BA5590 battery was significant at the temperatures of these tests.

B. GLLD Laser Designator Battery

The specifications for the above battery are as follows:

Dimension:	2.82" x 3.75" x 9.30"
Voltage:	Nominal 24V
	Maximum (OCV) 32V
	Average 24V
	End voltage 20V
Duty:	17.5A for 35.5 m.sec. followed by 1.8A for 14.5 m.sec. and the cycle continues for 3 minutes. This constitutes one burst. This 3 minute cycle occurs every 30 minutes.

The presently used Ni/Cd batteries provide 3 bursts per charge.

The voltage requirement of 32 volt necessitates the use of at least 8 Li/SOCl_2 D cells in series. The available battery volume can be occupied by 16 D cells. Therefore, the battery will consist of two D cells in parallel and 8 D cells in series, and a single D cell will experience half the specified constant current loads.

1. Testing of D Cells on Modified Duty Cycle:

We tested the Li/SOCl_2 D cells on a modified duty cycle involving an average current of 6.5A (13 A. for two cells in parallel) or 8A (in some cases) for 3 minutes every 27 minutes. This modified test consumes the same cell capacity per 3 minute burst as the above specified duty cycle. We used the modified duty cycle in order to expedite our cell development program since the test circuit for the specified duty cycle was still under development at this stage of the program. These tests were carried out to demonstrate the efficacy of the various current collector designs for the GLLD laser designator application.

One Li/SOCl_2 D cell with a cathode of design 2 (Table 1) having the tab located at the center of the 20 inch long electrode was tested under the modified GLLD duty cycle using a 6.5A current at room temperature. The voltage and the temperature of the cell were monitored during the three minute burst and are plotted as a function of burst number in Fig. 4. During each three minute 6.5A burst the cell voltage showed a slight recovery during the early stages of the discharge and a slight decline towards the end of the discharge. The cell temperature showed a sharp rise during the three minute burst and declined to almost the original level during the 27 minute open circuit stand. The cell delivered 16 bursts above 2.5 volt corresponding to a capacity of 5.2 A.hr. The cell temperature during the burst periods reached a maximum of 30°C which is well within the safe limits of temperature excursion. This cell was not insulated with glass filter paper.

A second D cell of similar construction was tested under the modified duty cycle using 8A and the cell was thermally insulated using glass filter paper. The test results are shown in Fig. 5. Note that the cell temperature rose to a maximum of 40°C towards the end of the discharge during the three minute 8A bursts. The cell delivered 12 bursts corresponding to a capacity of 4.8 A.Hr.

Another D cell of the same design was tested on the modified duty cycle using 6.5A bursts at -30°C . The results are shown in Fig. 6. Although the cell delivered 12 bursts, the cell voltage remained around 2.0 volt during most of the bursts.

One D cell with a 20 inch long cathode having both a horizontal and a vertical tab (design 4 of Table 1) was tested on the modified duty cycle using 6.5A bursts at room temperature. This cell was also thermally insulated with glass filter paper separator. The results are shown in Fig. 7. The cell delivered 10 bursts corresponding to a cell capacity of only 3.25 A.Hr. This low cell capacity is most likely due to the lower effective cathode area because of the presence of the horizontal tab.

One D cell with a 25 inch long cathode having one tab at one end (design 6 of Table 1) was tested on the modified duty cycle using 8A bursts at room temperature. The results are shown in Fig. 8. The cell showed unusually high polarization as well as a sharp rise in the cell temperature during the 3 minute bursts. The cell temperature reached a maximum of 55°C during the last burst. The cell only delivered 4 bursts above 2.0 volt. This poor performance may be attributed to the non-uniform current density distribution as a result of the poor current collection.

Two D cells with the 25 inch long cathode having both a horizontal and a vertical tab as in design 7 of Table 1 were tested on the modified duty cycle using 6.5A bursts at room temperature. The results from these two cells are shown in Fig. 9 and 10 respectively. The cells delivered 10 and 12 bursts corresponding to capacities of 3.25 and 3.9 A.Hr respectively. The maximum cell temperature remained below 40°C.

Another D cell of the same design was tested using 8A bursts at room temperature. The results are shown in Fig. 11. The cell delivered only 7 bursts corresponding to a capacity of only 2.8 A.Hr. Although the use of the horizontal tab leads to some improvement over the single vertical tab the improvements are only moderate because of the lowering of the active area by the horizontal tab.

Two D cells were made with 25 inch cathodes having two vertical tabs located equidistant from the cathode ends and the middle. One cell was tested on the modified duty cycle using 6.5A and the other one was tested using 8A at room temperature. The results are shown in Fig. 12 and 13 respectively. The cells delivered 16 bursts at 6.5A and 12 bursts at 8A corresponding to cell capacities of 5.2 and 4.8A.Hr respectively. This represents a significant improvement over the cells of the previous design.

Several D cells were made with 25 inch long cathodes having three tabs as in design 8 of Table 1. One cell was tested at room temperature on the

modified duty cycle using 6.5A. The results are shown in Fig. 14. The average cell voltage on load remained only slightly below 3 volts and was found to be rather stable. The cell temperature rose to a maximum of only 36°C during the 6.5A burst. The cell delivered 16 bursts above 2.5 volt corresponding to the cell capacity of 5.2 A.Hr.

Two D cells of the same design were tested at -30°C on the modified duty cycle using 6.5A current. The results are shown in Fig. 15 and 16 respectively. Note, that the average cell voltage on load was above 2.0 volt. The two cells delivered 10 and 8 bursts corresponding to the cell capacities of 3.25 and 2.6 A.Hr respectively. The performance of these cells was somewhat better than the cells of design 2 at -30°C.

Another D cell of the same design was tested at room temperature on a modified duty cycle using 8.75A. The results are shown in Fig. 17. The cell delivered 11 bursts and went into reversal during the 12th burst. The capacity delivered was 4.8 A.Hr.

This concludes all the testing of D cells on the modified duty cycle. The results (summarized in Table 2), indicate that the cells with 20 inch long cathodes having a tab in the middle provide adequate performance, it is also the simplest one to fabricate. The cells with 25 inch long cathodes with two or three tabs also performed satisfactorily. The use of horizontal tabs is not an efficacious and will not be considered for any further tests.

2. Testing of D Cells on Regular Duty Cycle

We designed and built test equipment capable of testing 8 batteries at one time on the GLLD Laser Designator duty cycle specified earlier. The test equipment was designed to draw constant currents of 17.5A and 1.8A for the desired time intervals from the battery down to a voltage of approximately 0.8 volt at which point the test is automatically terminated thus preventing any force-discharge on the cells. Since the GLLD battery will contain two D cells in parallel, we carried out the initial tests using two D cells in parallel instead of using the full 16 cell battery.

The D cells with 20 inch long cathodes having one tab in the middle (design 2) were tested at room temperature using the regular duty cycle. The results are shown in Fig. 18. The cell voltages on both the 17.5A and 1.8A loads are shown as a function of number of bursts. The two D cells delivered 9 bursts above 2.0 volts. On the 10th burst, the cell voltage on 17.5A dipped to 1.0 volt at which point the cell temperature rose sharply to 50°C. The test results of a second pair of D cells of the same design are shown in Fig. 19. In this case, the cells delivered 12 bursts. These results are approximately similar to the previous test results on the modified duty cycle.

The D cells with 25 inch long cathodes having three tabs (design 8) were tested at room temperature on the regular duty cycle. The results are shown in Fig. 20. The voltages on the first two bursts were not measured because of recorder malfunction. Note that the cell voltage on 17.5A was substantially above 2.5 volt and that the voltage remained quite stable during the 3 minute bursts. The two cells (in parallel) delivered 17 bursts corresponding to a total capacity of 11 A.Hr from the two D cells or 5.5 A.Hr/cell.

The above tests were repeated with another pair of the D cells of the same design. The results are shown in Fig. 21. In this test, the individual cells were covered with a heat shrinkable plastic jacket. The cell wall temperature was monitored during the test and it rose to a maximum of 40°C towards the end of the test. The cells delivered 18 bursts above 2.0 volt corresponding to a capacity of approximately 5.85 A.Hr/cell. This is approximately 50% of the total available cell capacity of 12 A.Hr. These results are extremely encouraging particularly in view of the fact that the presently used Ni/Cd batteries deliver only 3 bursts per charge.

C. Conclusions

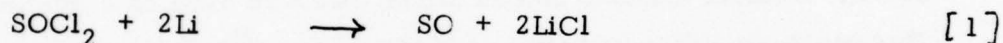
The rate capability of the Li/SOCl_2 D cells was increased substantially by improving the cathode designs. The cells with the improved cathodes were used to fabricate a BA5590 manpack radio battery containing 8 cells in series. The battery had a service life of 100 hrs at room temperature. This represents a 20% increase in service life with an associated weight saving of 11%

relative to the presently used Li/SO_2 BA5590 batteries which use 10 D cells.

The GLLD laser designator battery can accommodate 16 D cells which will be connected 8 in series and two in parallel. Li/SOCl_2 D cells of various cathode designs were tested on a prorated basis using single cell and two cells in parallel. The results showed that these batteries are capable of providing six times longer service life than do the currently used Ni/Cd batteries. The temperature of a single cell remained below 40°C during these high current tests.

III. Electrochemical and Spectroscopic Studies on SOCl_2 Reduction

Calorimetric (12) and DTA studies (7, 11) of Li/SOCl_2 D cells showed that chemical reactions continue to occur liberating heat after the discharge of the cell. Since these reactions do not occur in an undischarged cell, it is reasonable to assume that the reduction products of SOCl_2 are responsible, at least in part, for these spontaneous exothermal reactions. The reported spontaneous explosions of partially discharged Li/SOCl_2 cell on casual storage may also be initiated by the above unknown reactions involving the SOCl_2 reduction intermediates. Thus, knowledge regarding the nature of the unstable intermediates of SOCl_2 reduction may be useful as a guide for the improvement of the safety of the Li/SOCl_2 cells. We postulated (9, 13) the overall cell reaction to be



where SO may dimerize and then decompose to S and SO_2 or may form polymers. There is substantial evidence (5, 14) in favor of cell stoichiometry [1]. The quantitative formation of LiCl and qualitative formation of S and SO_2 are known. Very little has been known regarding intermediate species formed during the reduction of SOCl_2 . Attempts to use cyclic voltammetry (15, 16) in neat SOCl_2 - LiAlCl_4 solutions to study the discharge reaction were complicated by electrode passivation due to the precipitation of LiCl , insoluble in SOCl_2 . We have circumvented this electrode passivation problem by using a supporting electrolyte consisting of tetrabutylammonium hexafluorophosphate ($\text{N}(\text{C}_4\text{H}_9)_4\text{PF}_6$) in organic solvents such as dimethyl formamide (DMF) acetonitrile (AN), methylene chloride and dimethyl sulfoxide, for studying the SOCl_2 reduction. The electrode passivation is absent in the above solutions since both tetrabutylammonium chloride and S are soluble in the solvents studied. We carried out both cyclic voltammetry and coulometry in the above electrolytes and found that neither S nor SO_2 are formed as immediate reduction products. There exists at least one surprisingly long lived intermediate species which slowly decomposes to regenerate SOCl_2 . Our previous experiments have demonstrated a stoichiometry of 2.0 for the reduction of SOCl_2 .

We have examined the formation of this intermediate species and its reactions by a number of techniques, including high sweep rate cyclic voltammetry, UV-VIS spectroscopy and low temperature electrochemical studies. The results are reported below.

A. Experimental

Electrochemical experiments were performed using a PAR 173 potentiostat and PAR 175 function generator with associated ancillary equipment. Pulse polarograms were performed with a PAR 174A polarographic analyzer. The data were collected using conventional x-y and strip chart recorders. The data for fast sweep experiments were taken on a Tektronix model 5115 storage oscilloscope or a PAR 4101 scan recorder. Platinum working electrodes were pretreated by chromic acid followed by a wash with distilled water and air drying. Experimental solutions were routinely degassed with argon before the substrates were added. A silver chloride coated silver wire was used as a reference electrode. This electrode has a potential of 3.30V vs. Li in PF_6^- -DMF solutions. A $\text{Tl}^+\text{Hg}/\text{TlCl}_3$ reference electrode was used for the low temperature experiments in DMF.

The experiments were performed in cells of conventional design. The coulometric experiments were carried out in a two compartment H-cell using a glass frit to prevent passage of material from the working and auxiliary electrode compartments. The low temperature experiments were carried out using the jacketed cell in Figure 22.

The organic solvents were either Burdick & Jackson "Distilled in Glass" DMF, and CH_2Cl_2 or Eastman Spectro Grade acetonitrile or Aldrich "Gold Seal" Dimethyl Sulfoxide. The supporting electrolyte was prepared by metathesis of tetrabutylammonium chloride (TBACl) and lithium hexafluorophosphate in acetone/water and purified by multiple recrystallizations in hot ethanol.

B. Results

1. Cyclic Voltammetry

In addition to the solvents described earlier we have utilized dimethylsulfoxide (DMSO) because of its great ability to coordinate with and

thus stabilize highly reactive molecules.

A series of voltammograms for ~ 10 mM SOCl_2 in $\text{CH}_3\text{CN}/0.1$ N TBAPF_6 are shown in Fig. 23. In these voltammograms on a constant current scale of $25\mu\text{A}/\text{cm}$, the sweep rate, V , was varied from $0.20\text{V}/\text{sec}$ to $2.0\text{V}/\text{sec}$. As the sweep rate increases, the peak current increases, but an oxidation process near 0.0V appears at 500 mV/sec and becomes more prominent at 1.0 and $2.0\text{V}/\text{sec}$. The chemical entity which is being oxidized at this potential is not present in the solution originally since there is no anodic current at this potential until some of the thionyl chloride has been reduced. The sweep rate dependence of this oxidation wave shows that the species responsible for the oxidation is reacting fairly rapidly in solution. The oxidation and coupled reduction near $+1.0\text{V}$ is due to oxidation of chloride ion to chlorine. The chloride itself is generated by reduction of thionyl chloride.

The effect of concentration on the SOCl_2 reduction has been examined. Cyclic voltammograms of SOCl_2 at various concentrations at a Pt electrode are shown in Fig. 24. For a given sweep rate of 500 mV/sec the oxidation near 0.0V becomes less prominent as concentration increases. From the sweep rate dependence of this oxidation, we can conclude that the species responsible for this oxidation wave is reacting with thionyl chloride in solution or with itself. Change in the reduction behavior was also noted as the wave near -0.65V became less prominent and the one near -1.0V more prominent as the concentration increased.

We have also examined the effect of substrate changes on the thionyl chloride reduction. Ordinary graphite or porous carbon electrodes displayed too high a background current to be usable in these experiments. We have, however, examined the use of nickel, indium, gold, amalgamated gold, copper and silver as electrode materials for observing the SOCl_2 reduction. Cyclic voltammograms on nickel, iridium and gold electrodes were quite similar to those observed with Pt as shown in Fig. 25. The copper electrode showed a very limited area of usable voltage while the results with silver electrode are anomalous and reproduced in Fig. 26.

We have continued our work on the thionyl chloride reduction in DMF (and in AN) and the reduction appears to take place by the same mechanism. The better separation of the two reduction waves in DMF makes it a more attractive solvent for use in strictly electrochemical studies on this system. Experiments in which sweep rate and concentration were systematically varied in DMF/TBAPF₆ gave similar results for the reduction of SOCl₂ to those found in acetonitrile. The second reduction wave remained more prominent in DMF, suggesting that coordination with DMF was stabilizing the species responsible for the reduction process.

To examine the formation of the intermediate species more closely we also examined the reduction at higher sweep rates than usual, recording the current/voltage trace on a storage oscilloscope. At sweep rates as high as 100V/sec no qualitative change in the voltammogram could be observed. Except for uncompensated iR losses the voltammogram was similar to those generated at lower sweep rates. We were also able to use the storage oscilloscope with multiple sweeps of the same voltage range to examine the relationships of the two reduction waves and the oxidation near 0V. Using this method we were able to generate a "steady state" voltammogram of reduced thionyl chloride species. This voltammogram was quite unique (not shown because of the absence of photographic attachment) in that the first thionyl chloride reduction wave was absent while the second reduction wave and the oxidation near 0V were still present. This result indicates that the oxidation near 0.0+ does not regenerate thionyl chloride since the first reduction wave corresponding to the reduction of SOCl₂ is absent and as such the reduction of thionyl chloride is irreversible.

For further comparison we ran cyclic voltammograms in dimethylsulfoxide (DMSO), a solvent which is regarded as very good for reduced species because of its ability to stabilize reactive materials by complexation. DMSO is also known to have a rather low activity of residual water because of the sulfoxide's coordinating ability. A cyclic voltammogram for SOCl₂ in

DMSO/TBAPF₆ is shown in Fig. 27. The pattern of two successive reduction waves and an oxidation near 0.0V are very similar to that observed in DMF. The oxidation near 0.0V is quite prominent even at 0.05V/sec sweep rate, indicating that the reaction species involved is greatly stabilized by the DMSO solvent. The definition of the two reduction waves is very clear and there is little evidence for the appearance of the third wave near -1.0V which we noted in other solvents.

2. Coulometry

We have examined the coulometric reduction of SOCl_2 in DMF, acetonitrile, and methylene chloride. In all three solvents we have observed the regeneration of thionyl chloride by destruction of an intermediate species and have confirmed the Faradaic current of 2 equivalents of charge for each equivalent of SOCl_2 reduced. In particular, the reduction in acetonitrile is of interest since the UV-VIS solvent cutoff of 190 nm gives a much better spectral window than DMSO (268 nm), DMF (270 nm), or methylene chloride (230 nm). We were able to monitor the course of a coulometric reduction by using both cyclic voltammetry and UV-VIS spectroscopy to monitor changes in the solution. For comparative purposes, spectra of SCl_2 and S in acetonitrile are reproduced in Fig. 28 and 29, respectively. The wave lengths of maximum absorbance, 279 nm for SCl_2 and 277 for S are very similar to that of SOCl_2 , 277 nm as shown in Fig. 30, however, there is a second band in the spectrum near 234 nm which is not present in the spectra of SCl_2 and S. In this particular experiment 10 μl of SOCl_2 was used in 75 ml of CH_3CN to give a concentration of 1.83 mM SOCl_2 in CH_3CN . This concentration was experimentally determined to be usable for both cyclic voltammetry and UV-VIS spectroscopy. Changes in the cyclic voltammograms and spectra as a function of charge passed are displayed in Figs. 31 and 32. As the electrolysis proceeds, the absorbance maximum in the UV-VIS spectrum shifts from 277 to 291 nm corresponding to a lower energy. The absorbance also increases gradually with the electrolysis and reaches a maximum of 1.94 from 0.63. The absorbance then declines drastically to 0.79 at $n \approx 1.76$ (Fig. 33). The absorption peak at 290 nm disappears on storing the electrolyzed

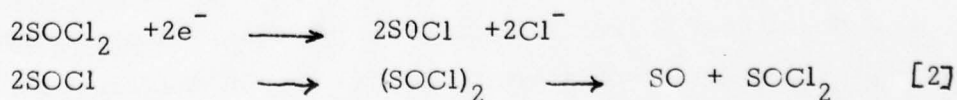
solution ($n \approx 2$) for one week at room temperature. At the same time, the first reduction wave in the cyclic voltammogram is destroyed and the second reduction wave becomes much more prominent. The UV-VIS spectra of the solutions after the electrolysis did not show the presence of S or SO_2 . When the solution was allowed to stand overnight the first wave became somewhat more noticeable and some poorly defined waves at more negative potentials also appeared. The final voltammograms showed two very poorly defined reduction waves with no SOCl_2 present, while the final spectra showed a substantial decline in absorbance.

C. Discussion

The coulometric data demonstrate an overall n value of 2.0 for the reduction of thionyl chloride. Reductions for extended times have given green, air-sensitive solutions possibly including polysulfides, but there is no evidence to suggest that this reflects any process occurring in SOCl_2 reduction since the cyclic voltammograms show that no further unreduced SOCl_2 is present.

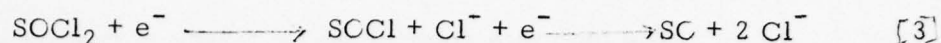
The spectroscopic evidence shows that S and SO_2 are not formed during the reduction process itself. Instead a different species is formed with an absorption band near 291 nm. This is confirmed by the cyclic voltammograms which show only a slow formation of species reducing at potentials near those for S and SO_2 . This intermediate species is reasonably stable and only slowly decomposes to generate more SOCl_2 .

We can now present a reasonable reduction mechanism for SOCl_2 which is supported by data at each stage. In an earlier report we suggested that the regeneration of SOCl_2 was due to destruction of a dimer formed by the coupling of one electron reduced species. [2]

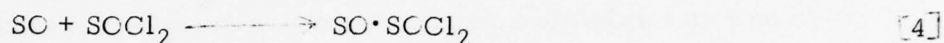


Our results from the high speed experiments make this seem less likely, since we were unable to outrun the dimerization process and observe two successive one electron reductions of SOCl_2 . The other mechanism we suggest now

seems the more likely of the two. In the initial reduction process, which gives the large waves in DMF and DMSC, there are two successive one electron processes to generate SC by a net two electron transfer [3] .



For reactions such as this, it is not unusual for E_0 for the second reduction process to be positive of E_0 of the first. Early in the reduction process SCCl_2 is present in large concentration compared to SC and reaction with SCCl_2 [4] is favored.



This species can slowly dissociate to regenerate SCCl_2 . As the electrolysis progresses the concentration of SC increases compared to SCCl_2 as reaction with SC is favored [5] .



The product $(\text{SC})_n$ is characterized by the absorbance near 291 nm and is reduced near -0.65V and the reduced product oxidized near +0.3V while the $\text{SC} \cdot \text{SCCl}_2$ product is oxidized near 0.0V as shown by the potential shift in this wave as the electrolysis continues. This species $(\text{SC})_n$ appears to be reasonably inert kinetically and only slowly decomposes to S and SC_2 , perhaps by loss of SC_2 to form successively oxygen deficient polymers. Observations of delayed pressure rise (19) and thermal activity (12) in discharged thionyl chloride cells are quite consistent with this hypothesis.

D. Conclusion:

Our data strongly suggest that there are at least two intermediate species formed in the reduction of SCCl_2 to LiCl, S and SC_2 . The decomposition of these species $\text{SC} \cdot \text{SCCl}_2$ and $(\text{SC})_n$ are probably responsible for the delayed SC_2 generation and thermal activity noted in discharged SCCl_2 cells.

IV. Conclusions and Future Work

The high rate spirally wound Li/SCCl_2 D cells showed considerable promise in both the BA5590 and the GLLD laser designator battery applications. Accordingly, we concentrated our effort on this area during the last two quarters. In view of the encouraging results obtained to date with the D cells we see no additional advantage in developing the 1.8 inch diameter cell which is exactly twice in volume of one D cell and as such we decided not to work on this for the time being. We began the design and the procurement of tooling for the fabrication of the 3 inch diameter flat cell (for the GLLD laser designator battery) during the first quarter. We plan to concentrate our effort on the development of this flat cell during the next quarter.

In addition, we plan to continue our work on the chemistry and the electrochemistry of the Li/SCCl_2 system in order to improve the safety of the system.

V References

1. W. K. Behl, J. A. Cristopulos, M. Ramirez and S. Gilman, J. Electrochem. Soc., 120, 1619 (1973).
2. J. J. Auborn, K. W. French, S. I. Lieberman, V. K. Shah and A. Heller, *ibid*, 120, 1613 (1973).
3. D. L. Maricle et al, U.S. Pat. 3, 567, 515 (1971); G. E. Blomgren and M. L. Kornenberg, German Pat. 2, 262, 256 (1973).
4. A. N. Dey and C. R. Schlaikjer, Proc. 26th Power Sources Symposium, Atlantic City, April 1974.
5. C. R. Schlaikjer, U.S. Pat. 4,020, 240 (1977), Proc. 28th Power Sources Symposium, Atlantic City, June 1978.
6. J. P. Gabano and P. Lenfant, Abstract No. 27, Electrochemical Society Meeting, Pittsburg, PA., Oct. 1978.
7. A. N. Dey, "Sealed Primary Lithium Inorganic Electrolyte Cell" Final Report, DELET-TR-74-0109-F, P. R. Mallory & Co., Inc., July 1978.
8. A. N. Dey and P. Bro., Proc. Brighton Power Sources Symposium (1976), p. 508.
9. A. N. Dey, J. Electrochem. Soc., 123, 1262 (1976).
10. A. N. Dey, J. Electrochem. Soc., (Communicated).
11. A. N. Dey, Proc. 28th Power Sources Symposium, Atlantic City, June 1978.
12. P. Bro, J. Electrochem. Soc., 125, 674 (1978).
13. A. N. Dey, Thin Solid Films, 43, 131 (1977).
14. D. R. Cogley and M. J. Turchan, "Lithium-Inorganic Electrolyte Batteries," Second Quarterly Report; ECOM-74-0030; AD 779477 EIC Inc., May 1974.
15. W. K. Behl, in "Proceedings of the 27th Power Sources Symposium," Atlantic City, N.J., June 1976.
16. G. E. Blomgren, V.Z. Leger, M. L. Kronenberg, T. Kalnoki-Kis and R. J. Brodd, in "Proceedings 11th International Power Sources Symposium," Brighton, England, 1978.
17. R. N. Adams "Electrochemistry at Solid Electrodes," Dekker (1969).
18. P. W. Schenk and R. Steudel, Angew. Chem. Internat. Edit. 4, 402 (1965).

19. M. Domeniconi, K. Klinedinst, N. Marincic, C. Schlaikjer, R. Staniewicz and L. Swette, "Inorganic Electrolytes," Office of Naval Research; Interim Report, Contract #N00014-76-C-0524; GTE Laboratories; Jan. 1976 to Oct. 1977.
20. R. P. Martin, Thesis "The Electrochemical Reduction of Sulfur Dioxide and of Elemental Sulfur in Nonaqueous Solvents," University of California, March 1973.
21. A. N. Dey, W. Bowden, J. Miller, P. Witalis, "Lithium-Thionyl Chloride Battery", ERADCOM, DELET-TR-78-0563-1, First Quarterly Report, P. R. Mallory & Co. Inc., April, 1979.

TABLE 1

Short-Circuit Currents of Hermetic D Cells with Various Cathode Designs

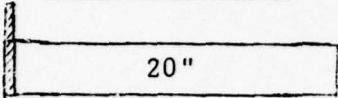
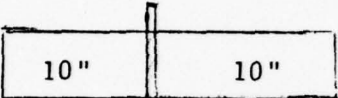
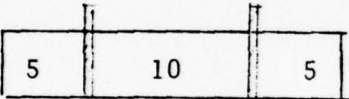
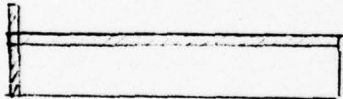
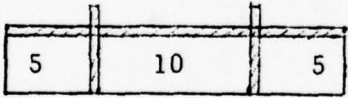
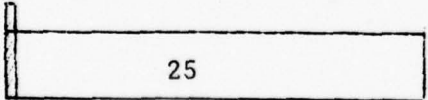
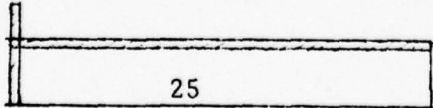

<u>No.</u>	<u>Cathode Designs</u>	<u>Maximum Short Circuit</u>	
		Current (A)	Current Density (mA/cm ²)
1.	 20"	24	53
2.	 10" 10"	76	168
3.	 5 10 5	94	208
4.	 25	58	128
5.	 5 10 5	98	217
6.	 25	35	62
7.	 25	65	115
8.	 12-1/2 12-1/2	104	184

TABLE 2
Behavior of High Rate Li/SCCl₂ D Cells on GLLD Modified Duty Cycle

Cathode Designs	Current	Duty Cycles above 2.0 volt	Test Temp.
	6.5A	10	25° C
	6.5A	10	25° C
	8	7	25° C
	6.5A	12	25° C
	8	4	25° C
	6.5A	16	25° C
	8	11	25° C
	6.5"	0 (11)*	-30° C
	6.5A	16	25° C
	8 A	12	
	6.5A	8 (11)*	-30° C
	6.5	10 (13)*	-30° C
	6.5	16	25° C
	8.75A	11	25° C

* Number of cycles before the cell entered voltage reversal.

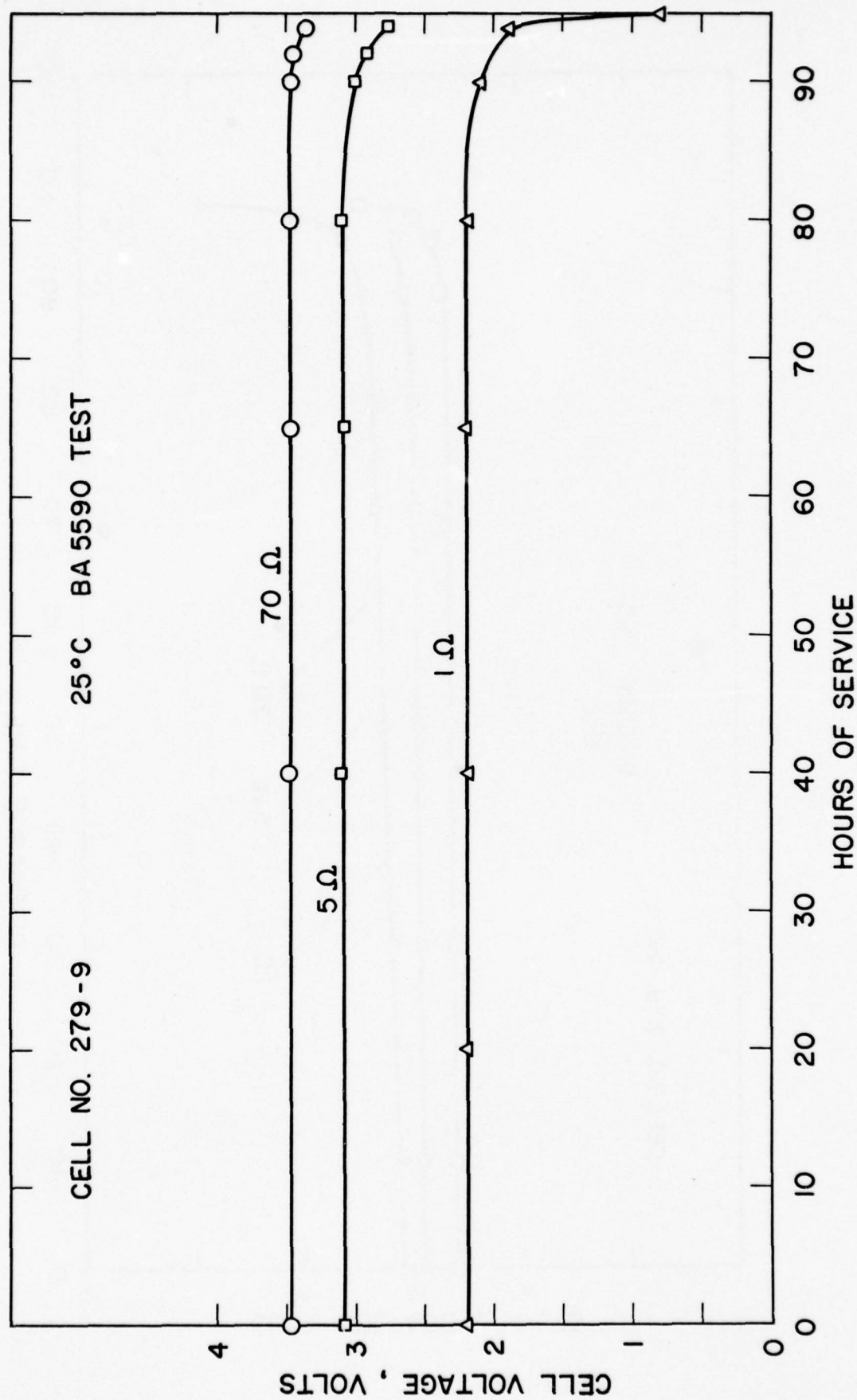


Fig. 1 Performance of high rate Li/SCCl₂ D cell on prorated BA5590 test at 25°C

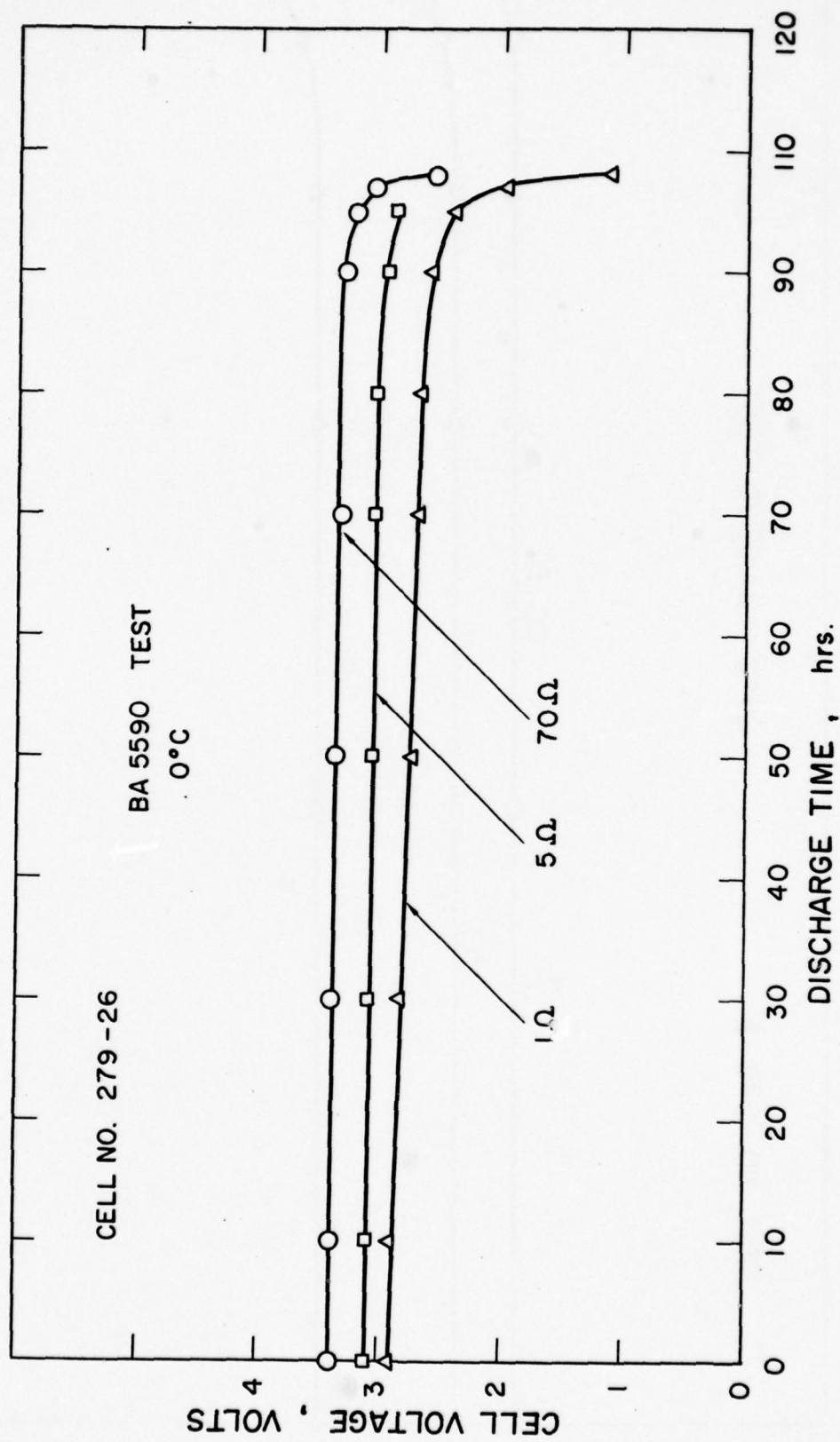


Fig. 2 Performance of high rate Li/SCCl₂ D cell on prorated BA5590 test at 0°C

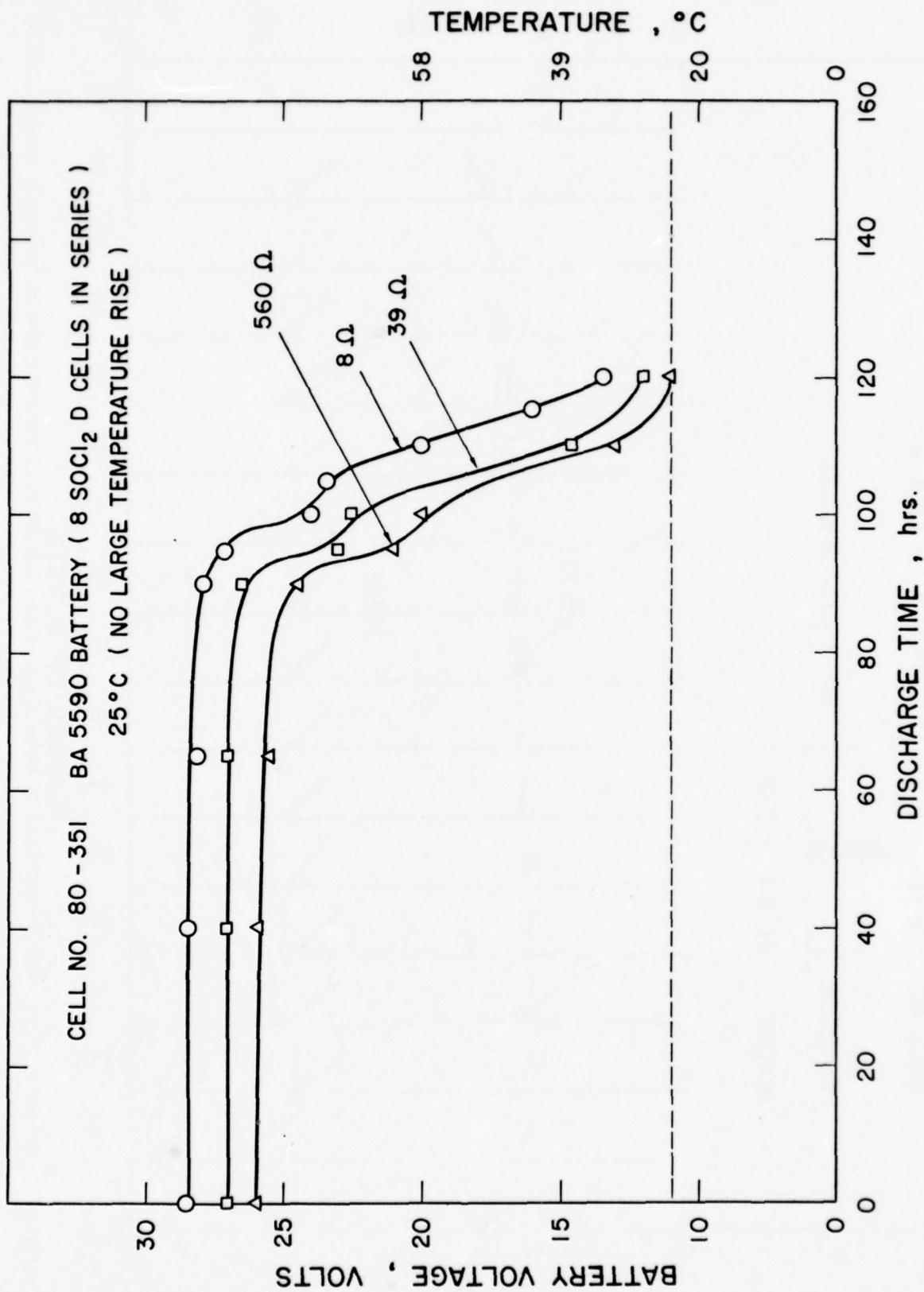
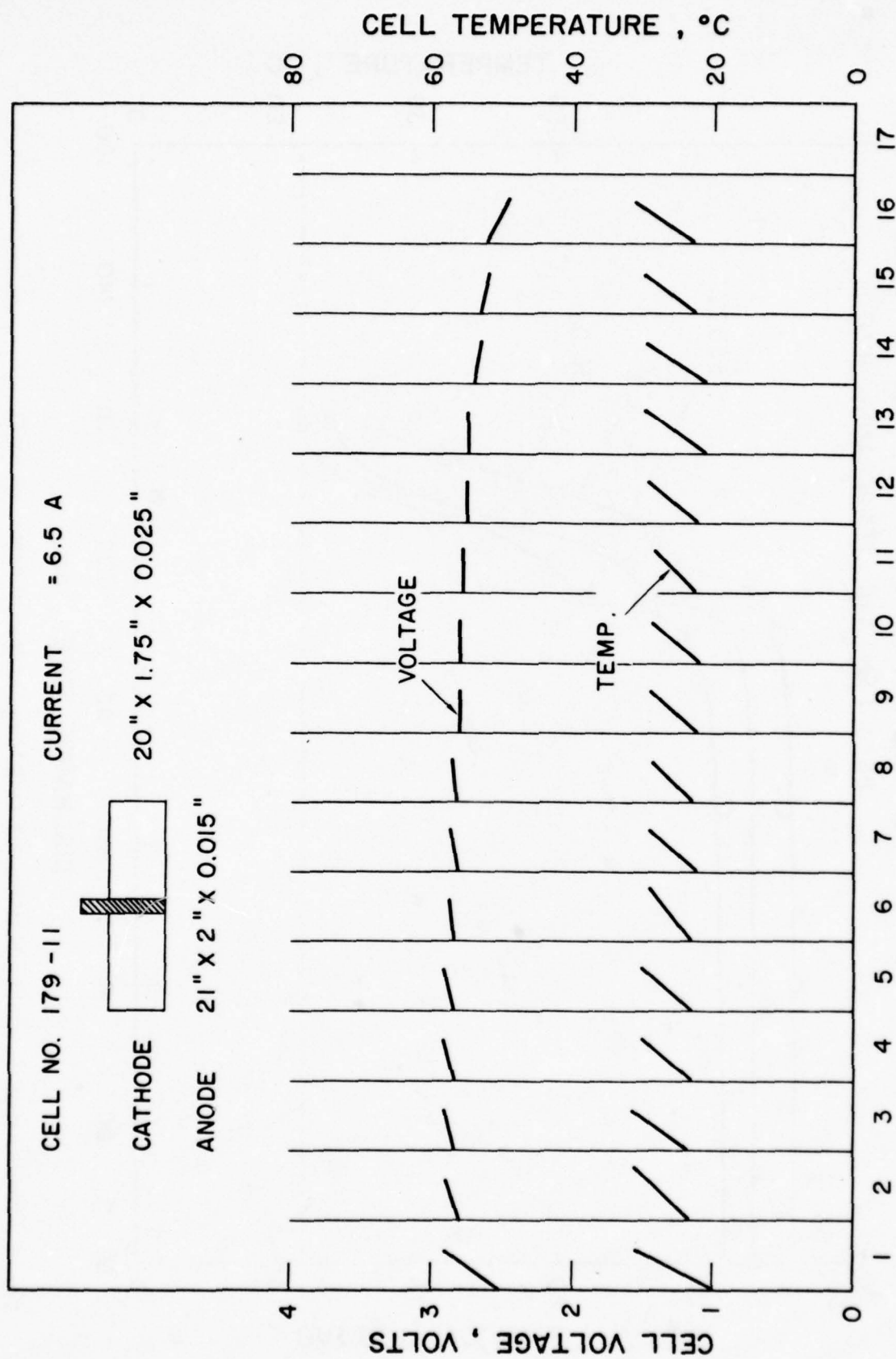
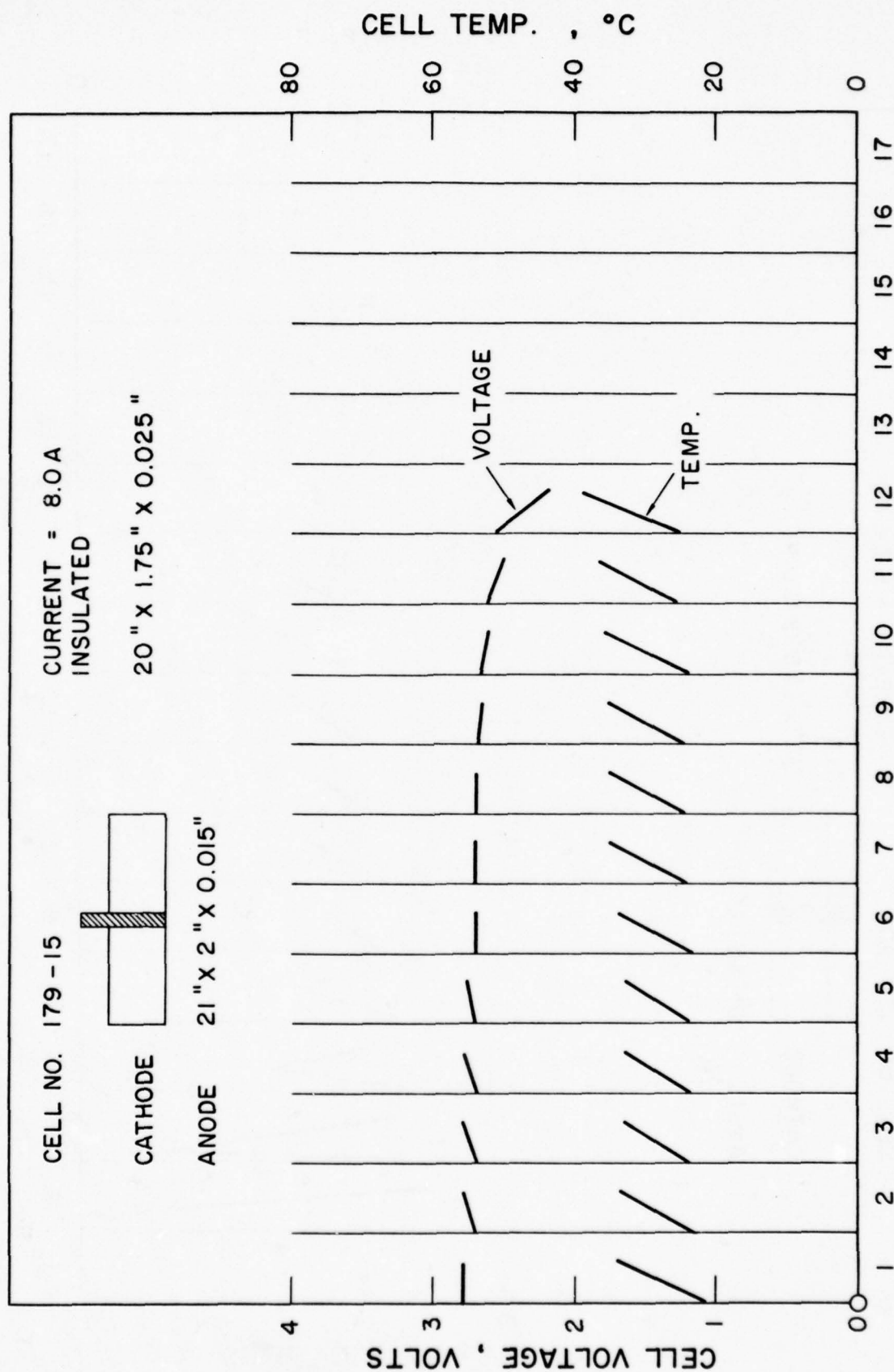


Fig. 3 Performance of BA5590 battery of 8 Li/SOCl_2 D cells in series at 25°C



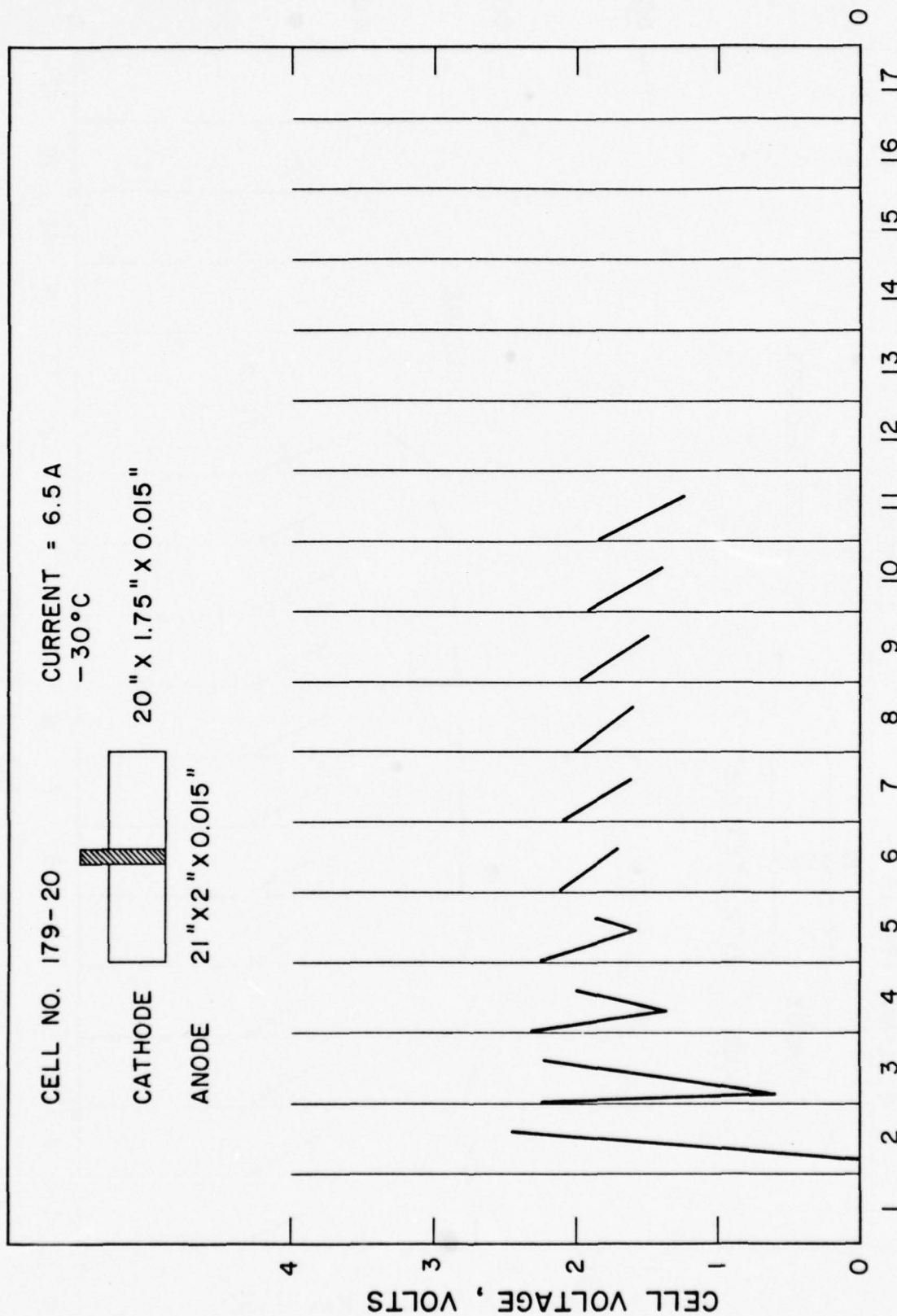
NUMBER OF BURSTS

Fig. 4 Voltage and temperature profiles of Li/SCl₂D cell with 20 inch carbon cathode having a central tab on modified GLID test consisting of 6.5A pulse of 3 minute duration every 27 minutes at 25°C



NO. OF BURSTS

Fig. 5 Voltage and temperature profiles of an insulated Li/SCCl₂ D cell with 20 inch carbon cathode having a central tab on modified GLLD test consisting of 8.0A pulse of 3 minute duration every 27 minutes at 25°C



NO. OF BURSTS

Fig. 6 Voltage profiles of Li/SCCl₂ D cell with 20 inch cathode having a central tab on modified GLLD test consisting of a 3 minute 6.5A pulse every 27 minutes at -30°C

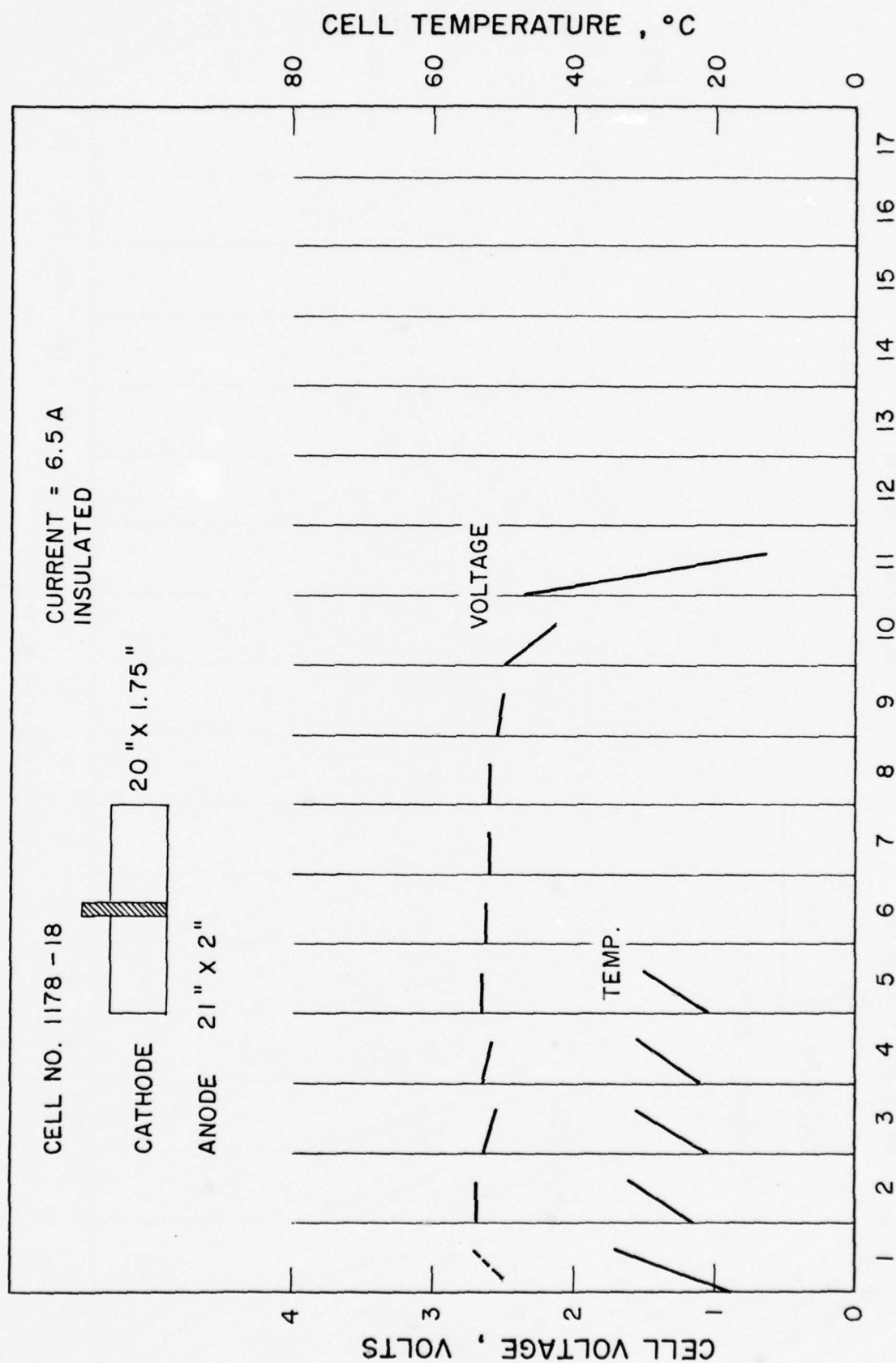


Fig. 7

Voltage and temperature profiles of an insulated Li/SOCl₂ L cell with 20 inch cathode having both a horizontal and vertical tab on modified GLID test consisting of a 3 minute 6.5A pulse every 27 minutes at 25°C

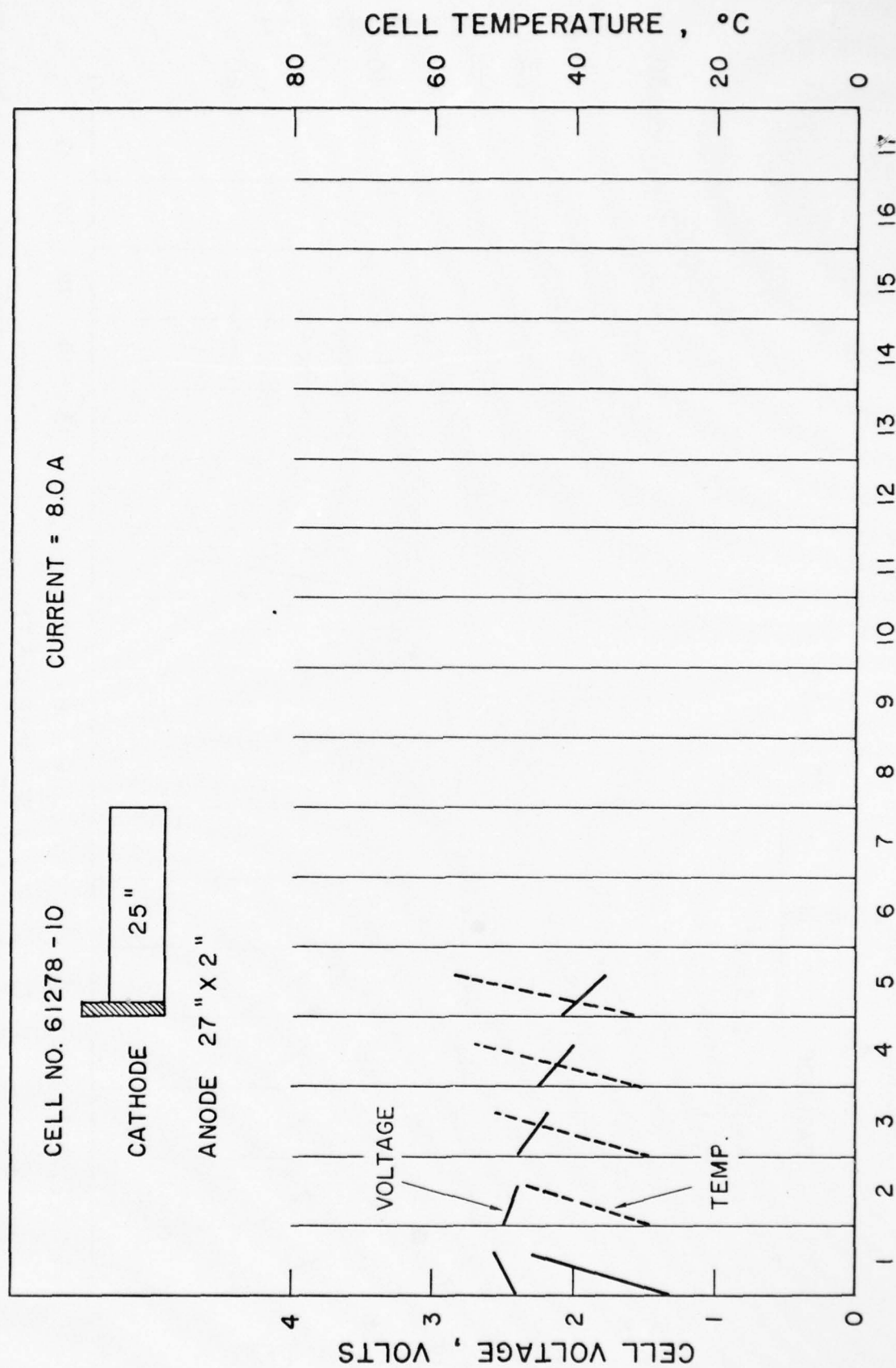


Fig. 8 Voltage and temperature profiles of Li/SCCl₂ D cell with 25 inch cathode having one tab at one end on the modified GLLD test consisting of a 3 minute 8A pulse every 27 minutes at 25°C

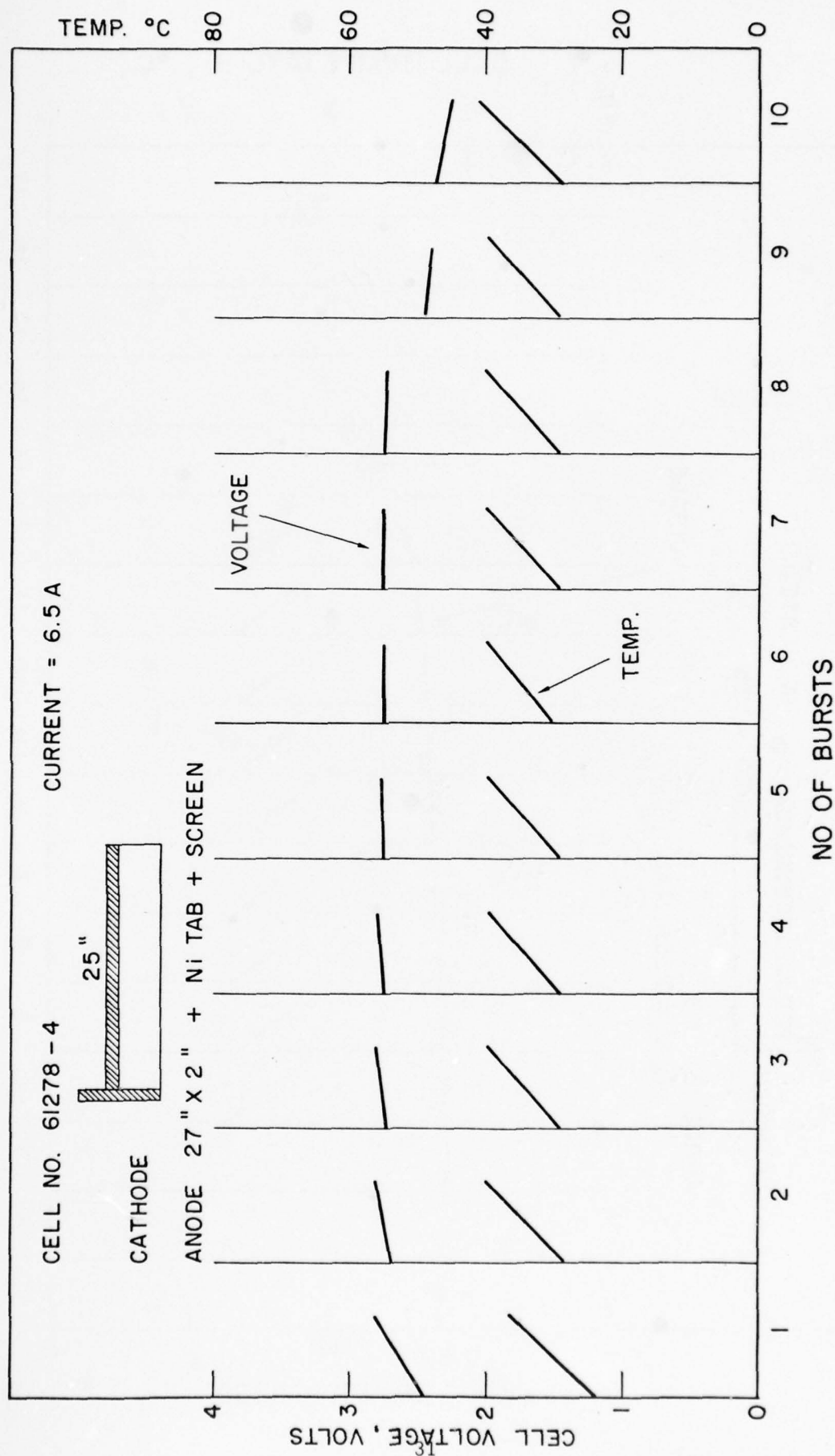


Fig. 9 Voltage and temperature profiles of Li/SCCl₂ D cells having 25 inch cathode with both a horizontal and a vertical tab on modified GLLD test consisting of a 3 minute 6.5A pulse every 27 minutes at 25°C.

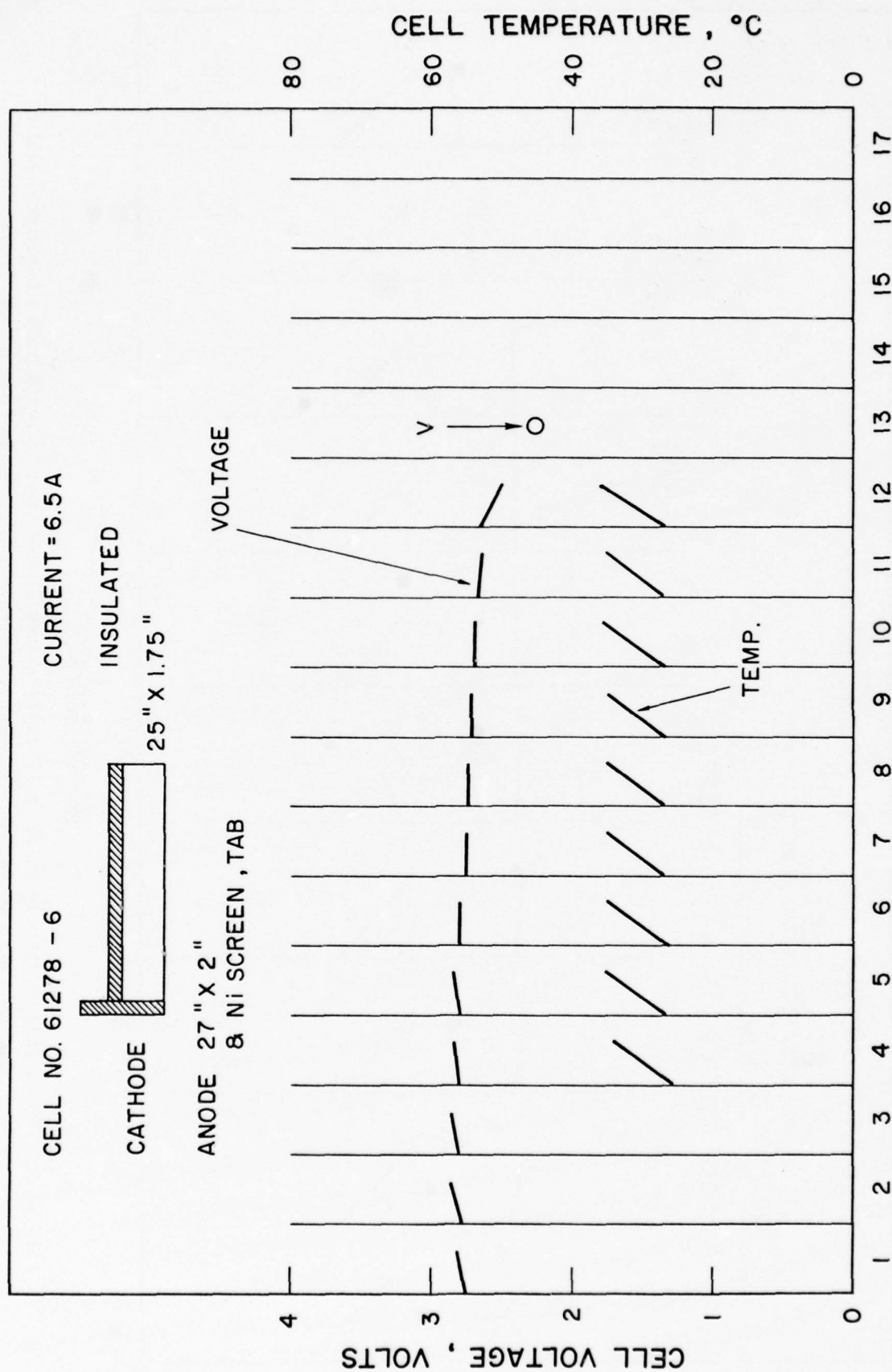


Fig. 10 Voltage and temperature profiles of an insulated Li/SCCl_2 D cell with 25 inch cathode having both a horizontal and a vertical tab on modified GLLD test consisting of a 3 minute 6.5A pulse every 27 minutes at 25°C

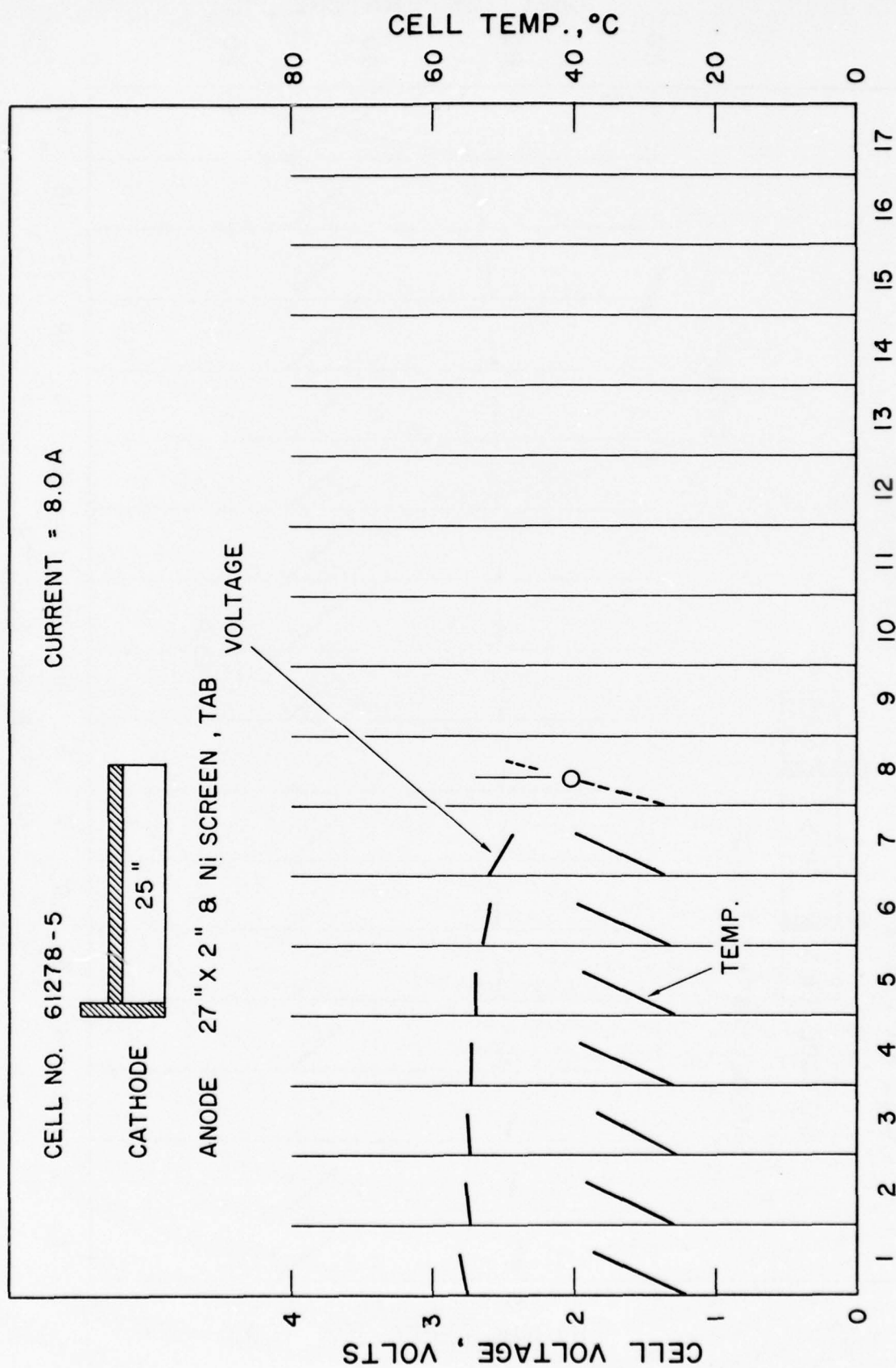


Fig. 11 Voltage and temperature profiles of a Li/SOCl₂ D cell with 25 inch cathode having both a horizontal and a vertical tab on the modified GLID test consisting of a 3 minute 8A pulse every 27 minutes at 25°C

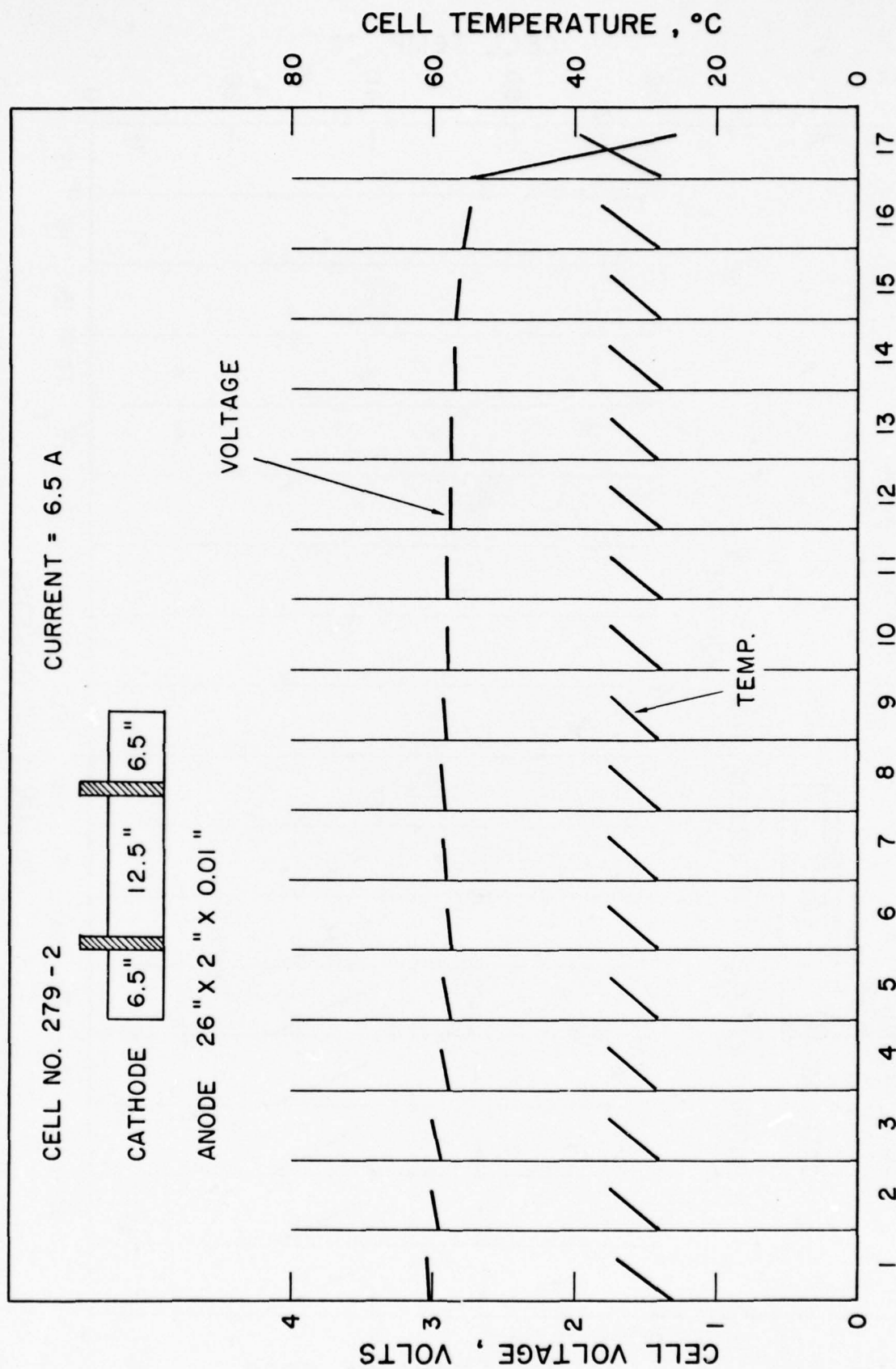
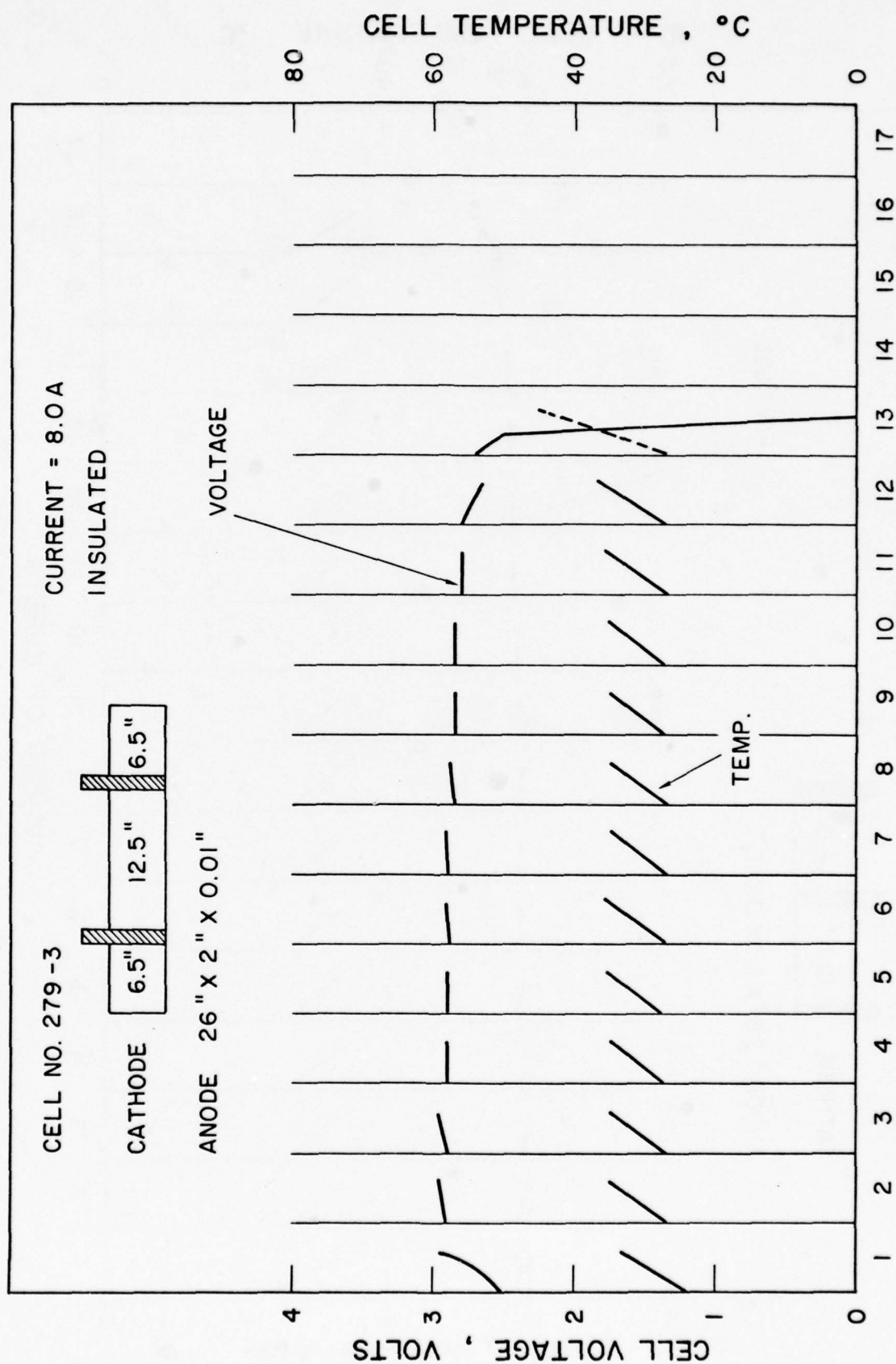


Fig. 12 Voltage and temperature profiles of an insulated Li/SOCl₂ D cell with 25 inch cathode having two tabs on the modified GLLD test consisting of a 3 minute 6.5A pulse every 27 minutes at room temperature



NUMBER OF BURSTS

Fig. 13 Voltage and temperature profiles of an insulated Li/SCCl₂ D cell with 25 inch cathode having two tabs on the modified GLLD test consisting of a 3 minute 8.0A pulse every 27 minutes at room temperature

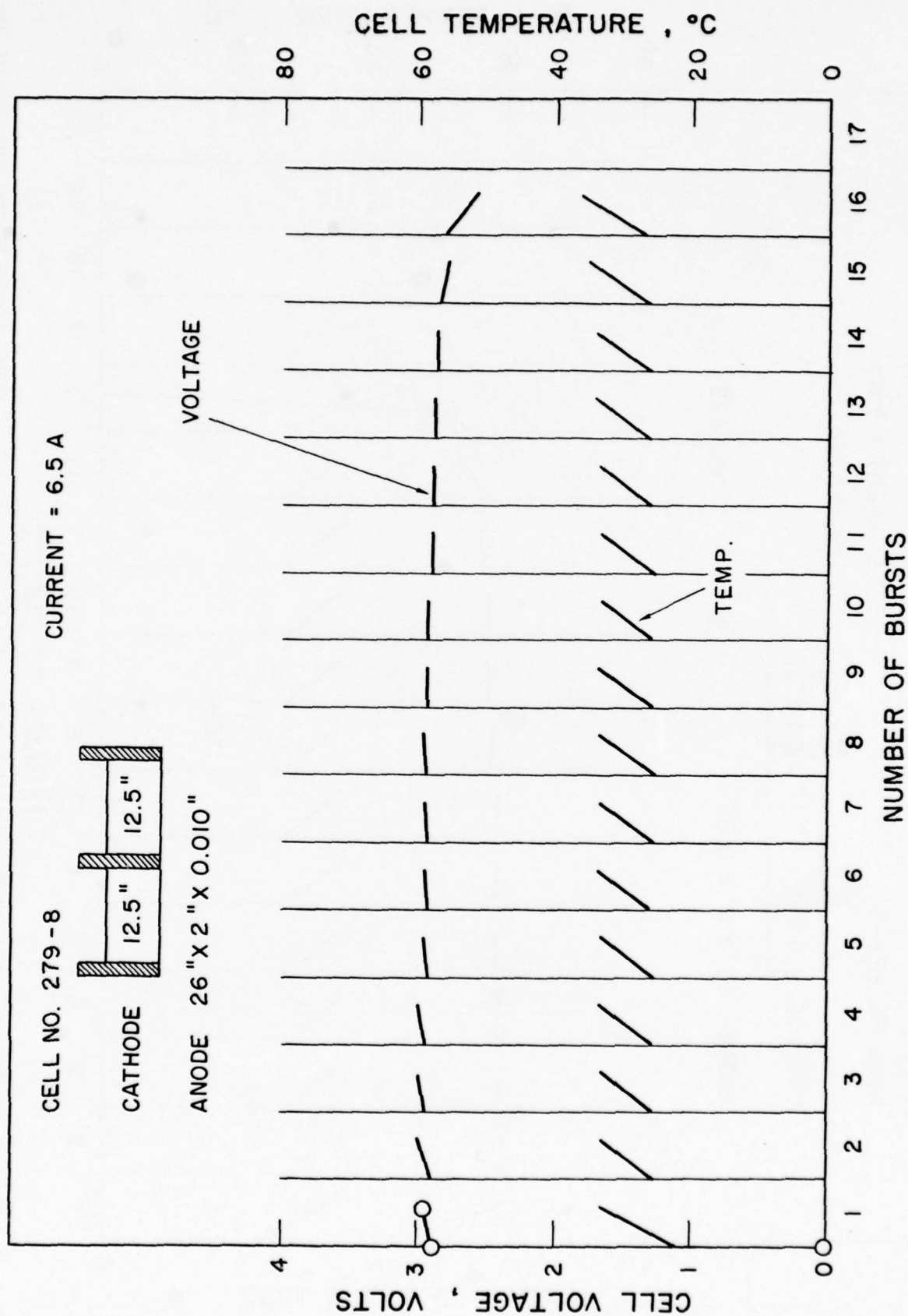


Fig. 14 Voltage and temperature profiles of a Li/SCCl₂ D cell with 25 inch cathode having three tabs on the modified GLLD test consisting of a 3 minute 6.5A pulse every 27 minutes at room temperature

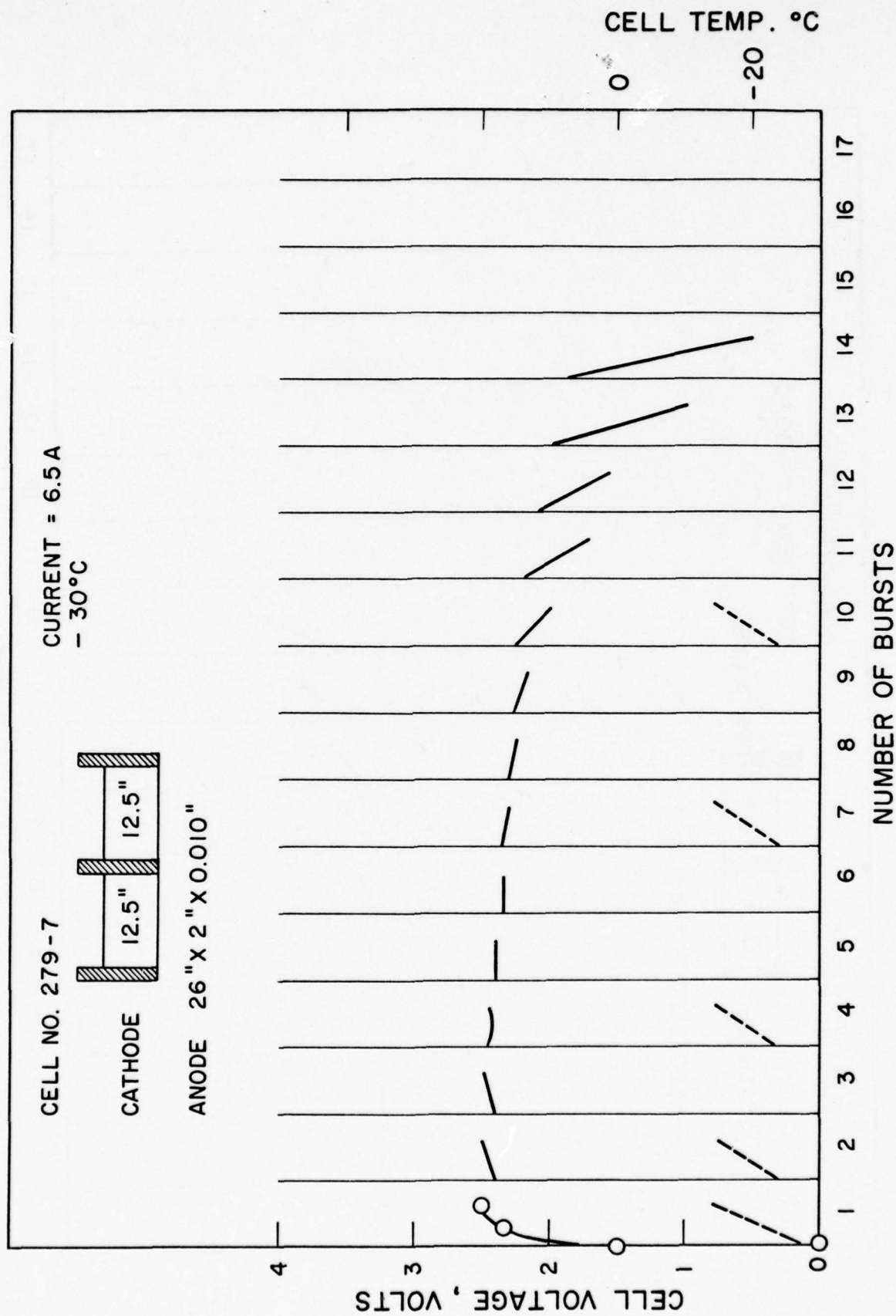
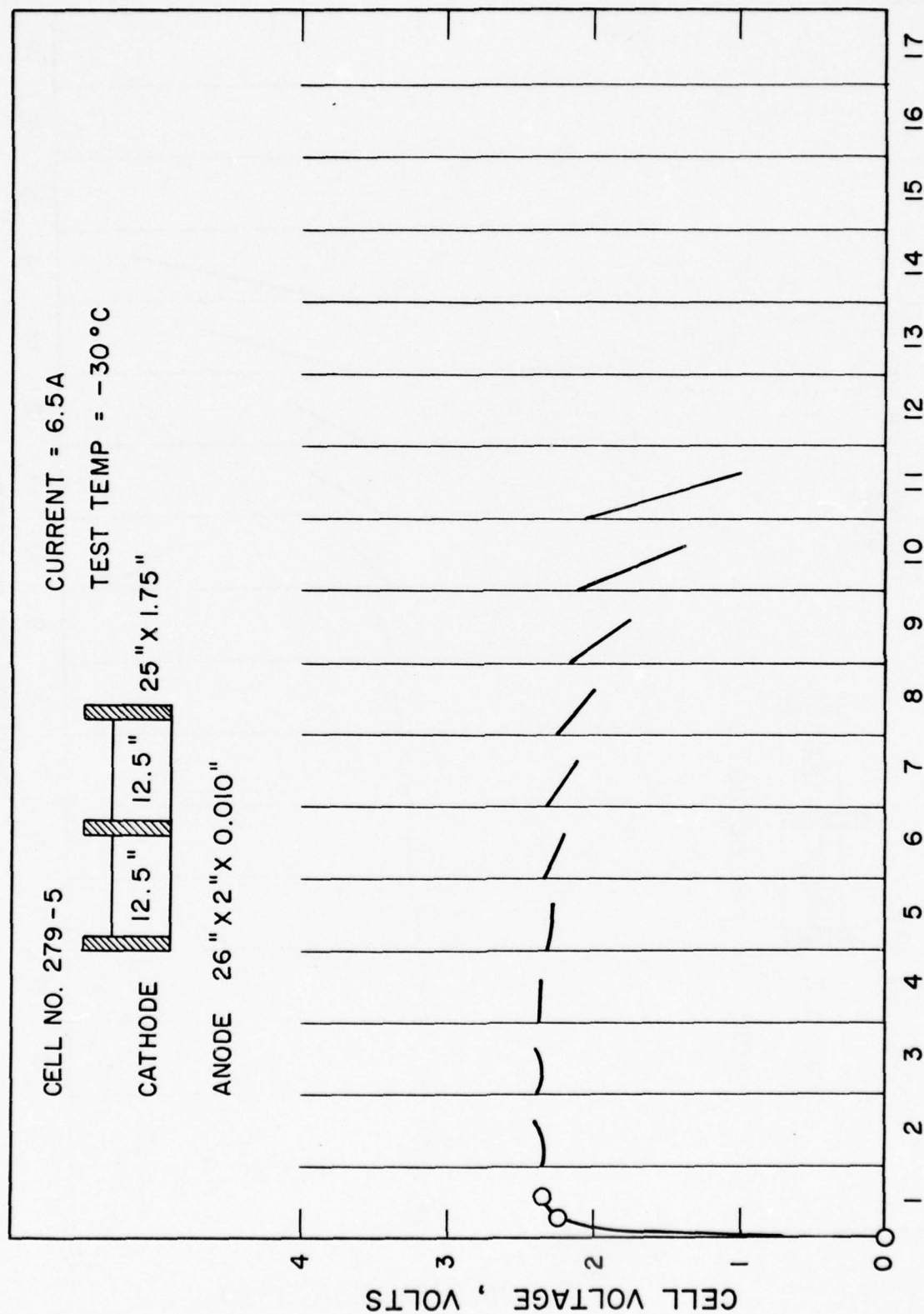


Fig. 15 Voltage and temperature profiles of a Li/SCCl₂ D cell with 25 inch cathode having three tabs on the modified GLID test consisting of a 3 minute 6.5A pulse every 27 minutes at -30°C



NO. OF BURSTS

Fig. 16 Voltage and temperature profiles of a Li/SCCl_2 D cell with 25 inch cathode having three tabs on the modified GLLD test consisting of a 3 minute 6.5A pulse every 27 minutes at -30°C

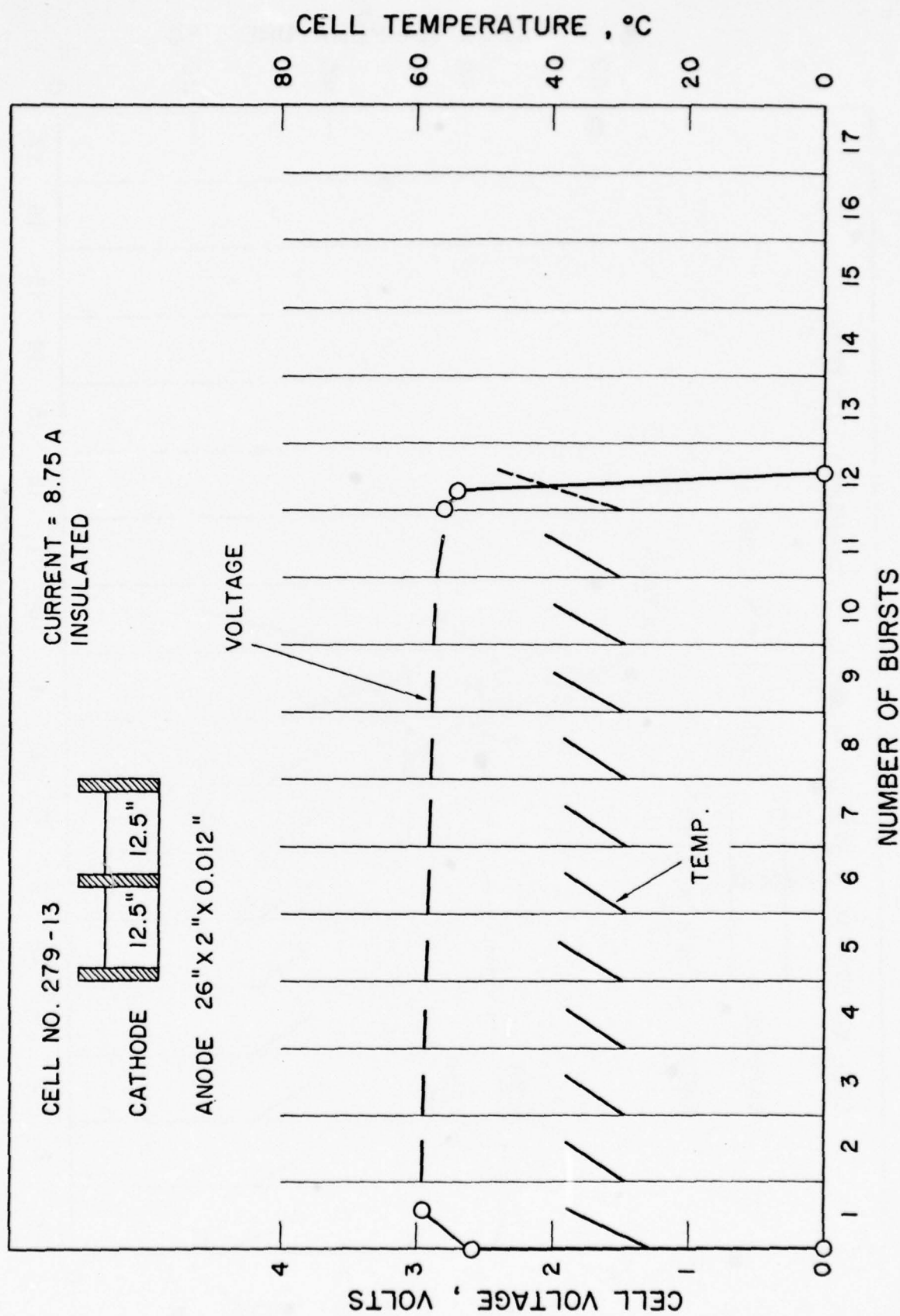


Fig. 17 Voltage and temperature profiles of an insulated Li/SCl₂ D cell with 25 inch cathode having three tabs on the modified GLLD test consisting of a 3 minute 8.75A pulse every 27 minutes at room temperature

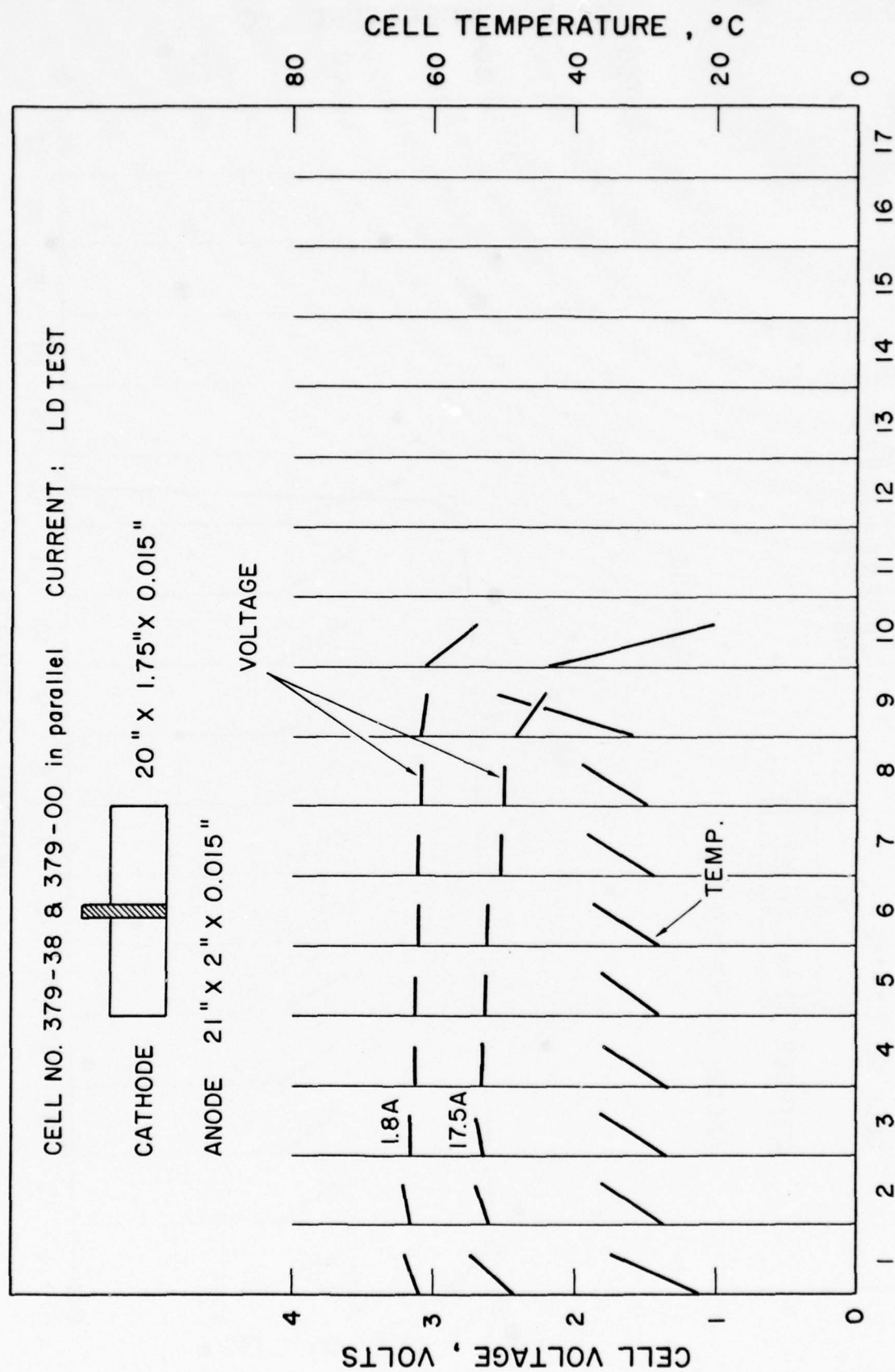


Fig. 18 Voltage and temperature profiles of two parallel connected Li/SCCl_2 D cells with 20 inch cathode having one tab located at the center of the actual GLID test involving 17.5A and 1.8A consecutive pulses for 3 minutes every 27 minutes at room temperature

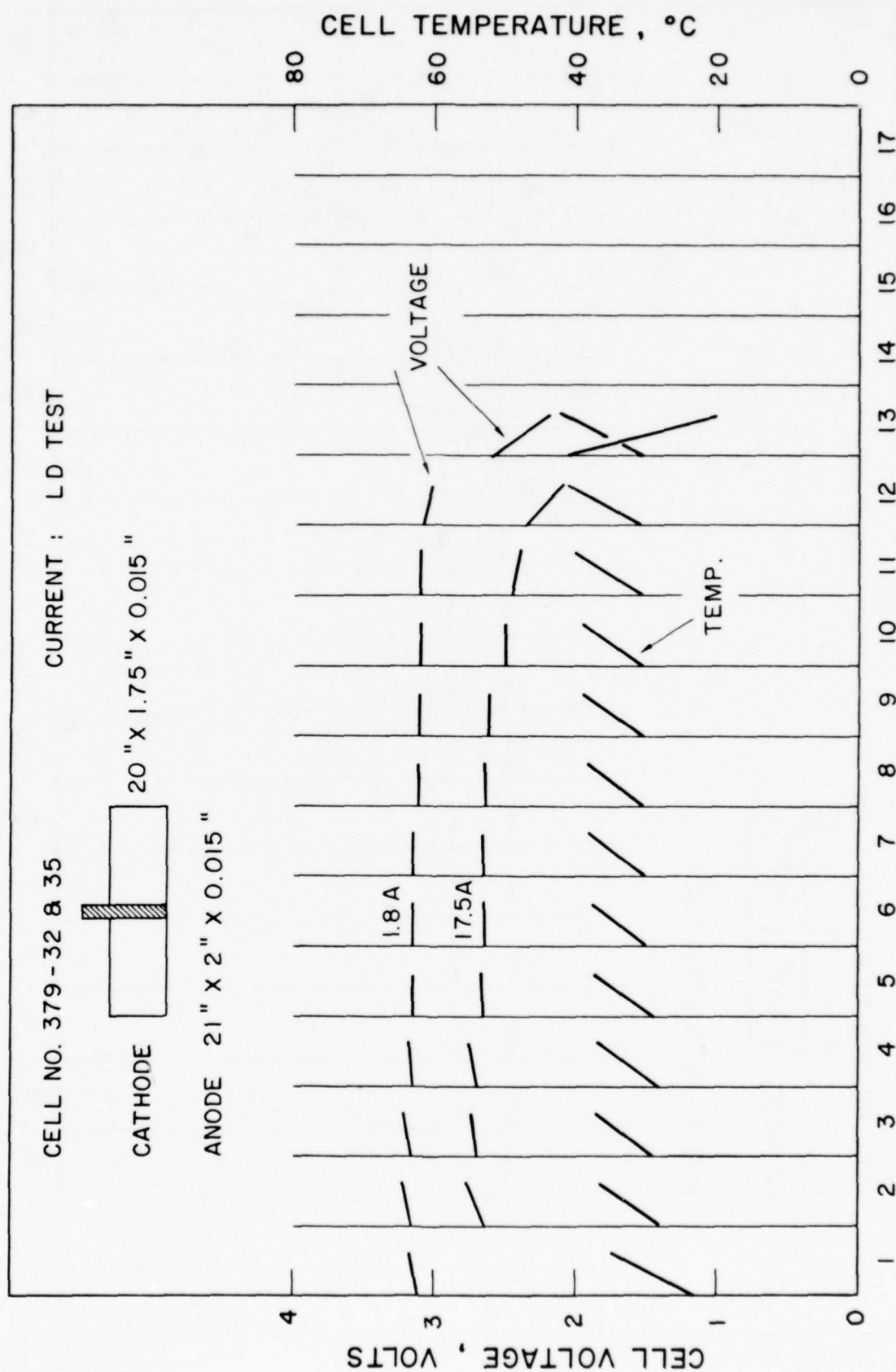


Fig. 19 Voltage and temperature profiles of two parallel connected Li/SOCl_2 D cells with 20 inch cathode having one tab located at the center on the actual GLLD test involving 17.5A and 1.8A consecutive pulses for 3 minutes every 27 minutes at room temperature

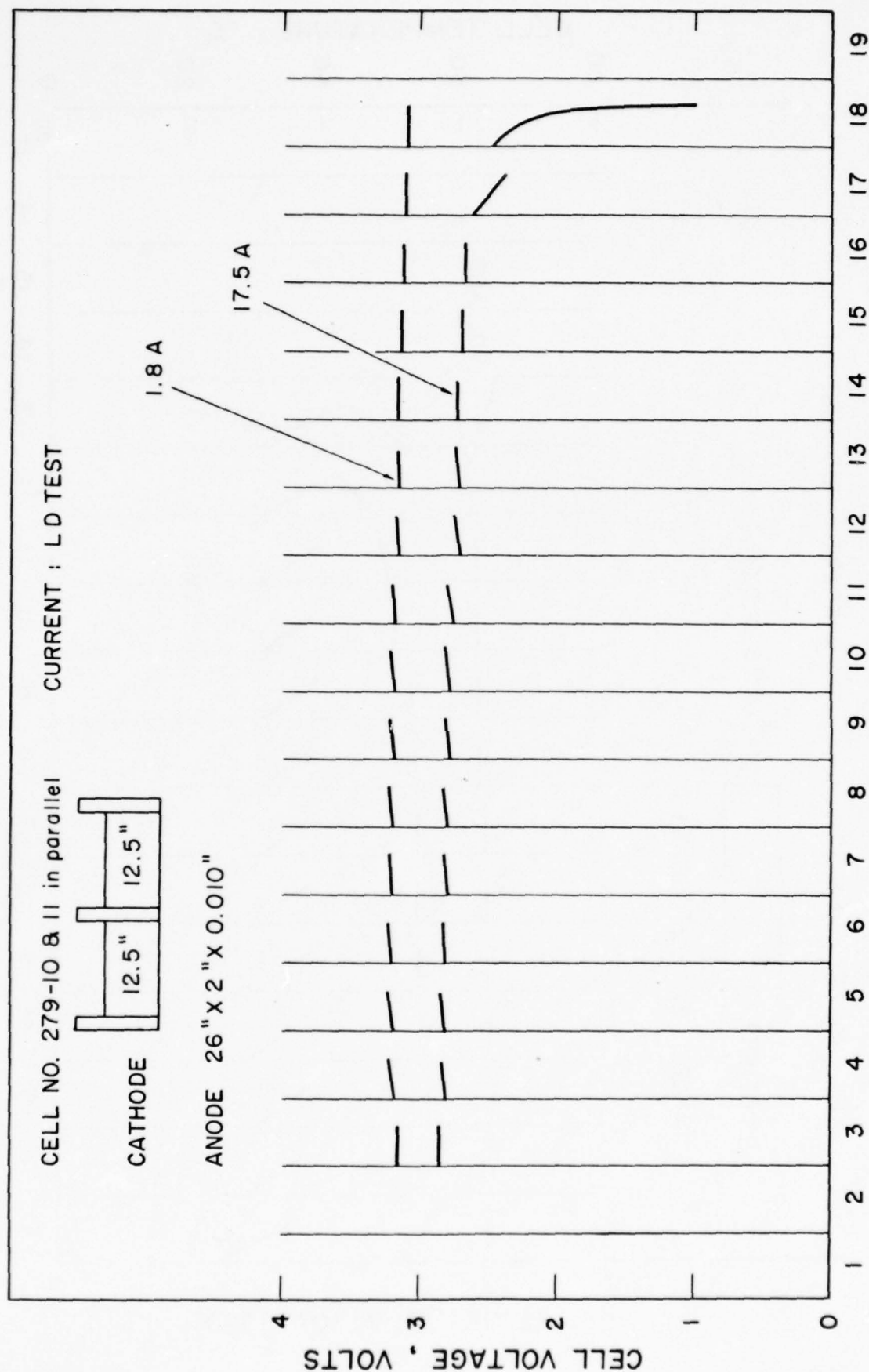


Fig. 20 Voltage and temperature profiles of two parallel connected Li/SCCl₂ D cells with 25 inch cathode having three tabs on actual GLLD test involving 17.5A and 1.8A consecutive pulses for 3 minutes every 27 minutes at room temperature

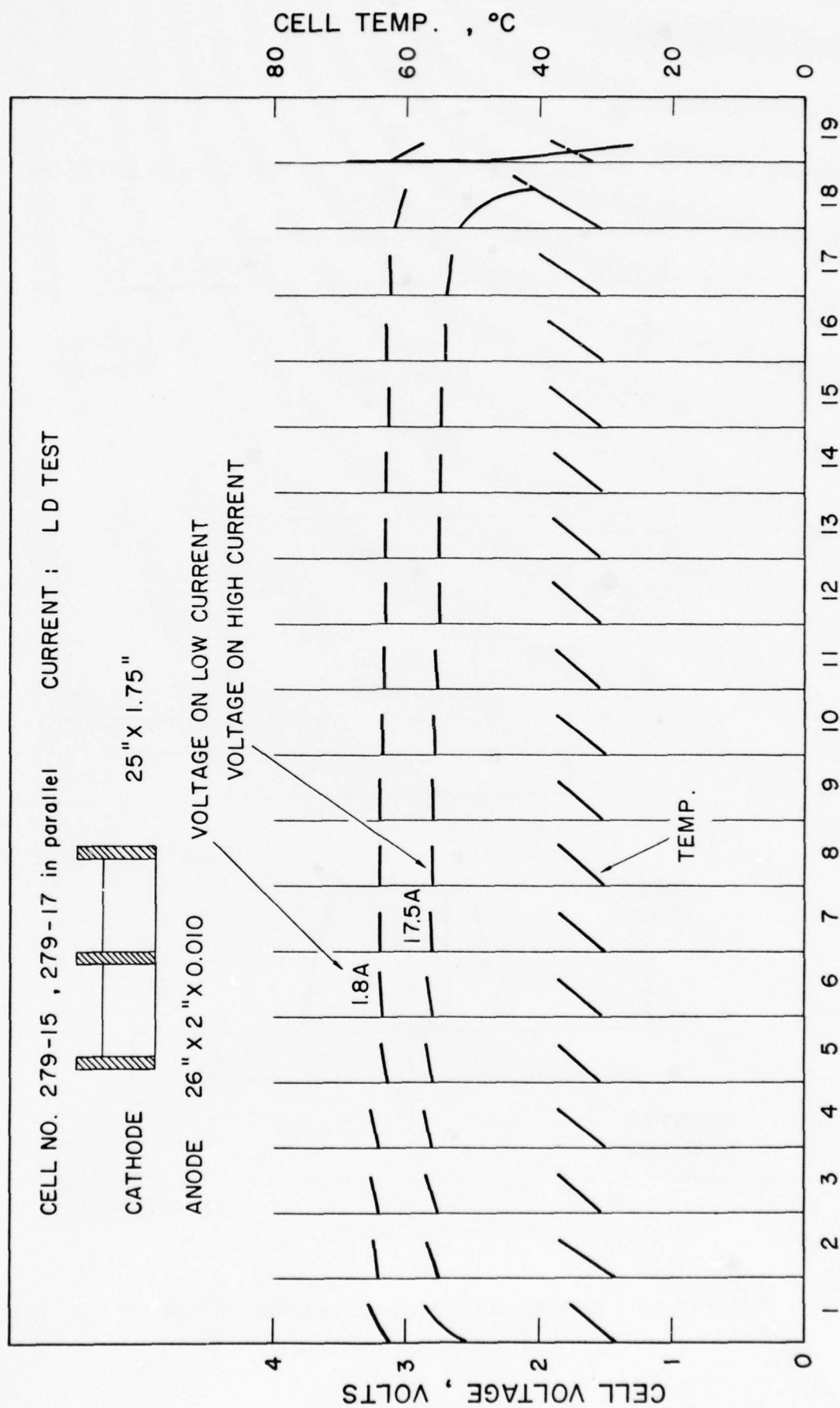


Fig. 21 Voltage and temperature profiles of two parallel connected Li/SCCl₂ D cells (with heat shrinkable jackets) with 25 inch cathode having three tabs on actual GLLD test involving 17.5A and 1.8A consecutive pulses for 3 minutes every 27 minutes at room temperature

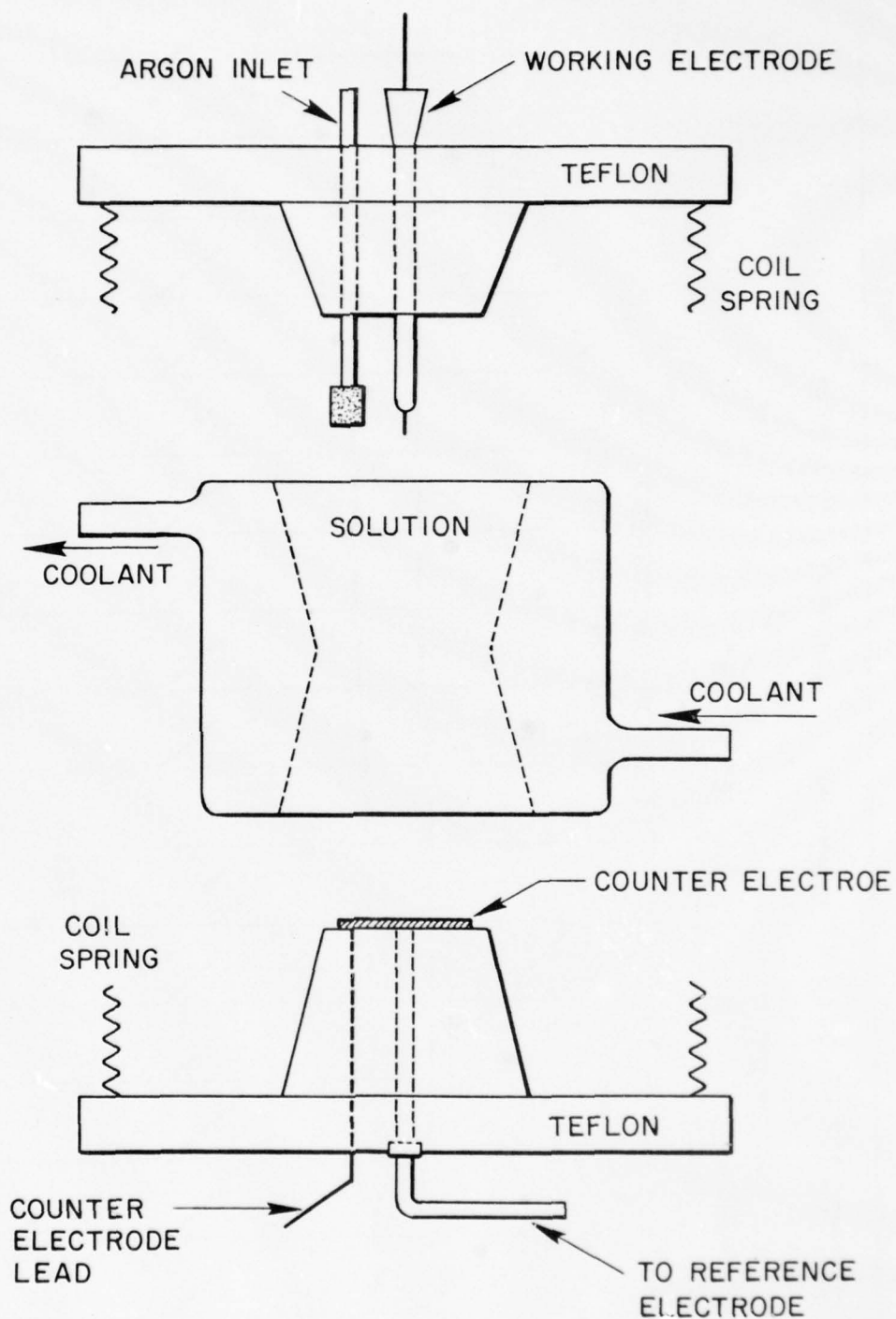


Fig. 22 Schematic drawing of the jacketed cell used for cyclic voltammetry at various temperatures

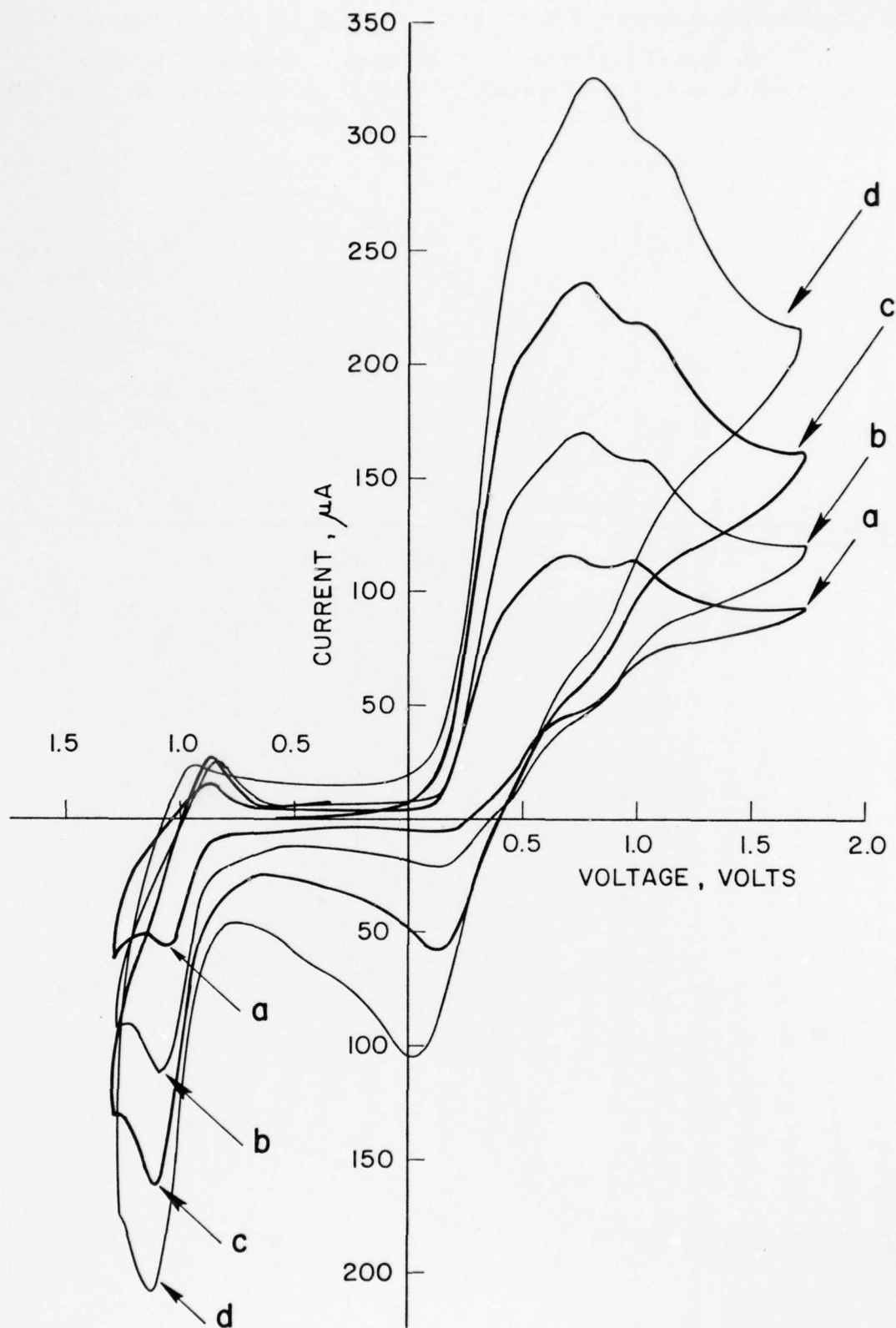
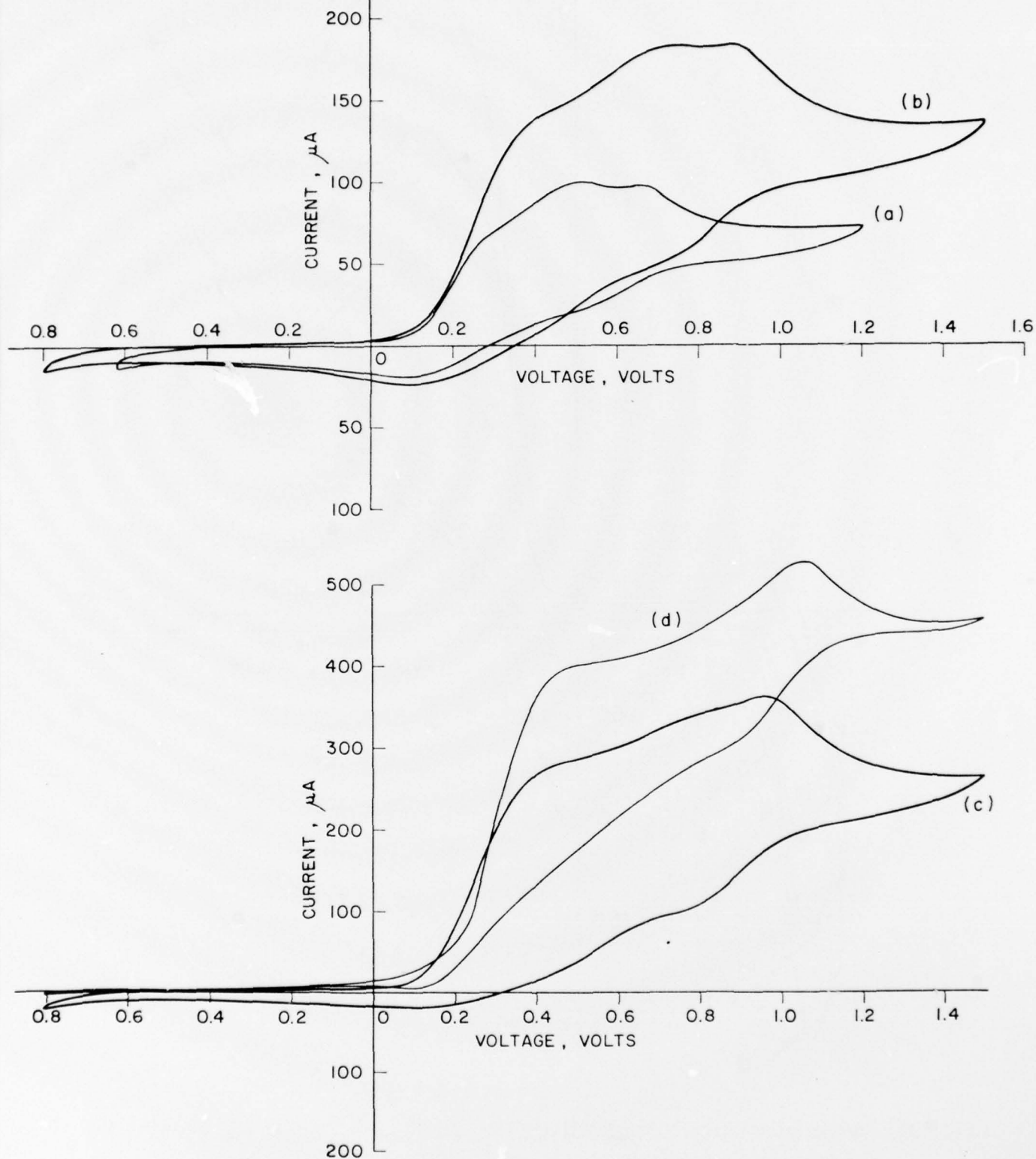


Fig. 23 Cyclic voltammogram of SOCl_2 in $\text{CH}_3\text{CH}/0.1\text{N N}(\text{C}_4\text{H}_9)_4 \text{PF}_6$ showing the effect of sweep rate at a Pt wire electrode
 a) 0.20 V/sec b) 0.50 V/sec c) 1.0 V/sec d) 2.0 V/sec

Fig. 24 Cyclic voltammograms of SCCl_2 in $\text{CH}_3\text{CN}/\text{N}(\text{C}_4\text{F}_9)_4\text{PF}_6$ at various concentrations

a) $25\mu\text{l SCCl}_2/75\text{ ml}$ (V 0.50 V/sec, b) $50\mu\text{l SCCl}_2/75\text{ ml}$ (V 0.050 V/sec), c) $100\mu\text{l SCCl}_2/75\text{ ml}$ (V 0.20 V/sec, d) $200\mu\text{l SCCl}_2/75\text{ ml}$ (V 0.20 V/sec).



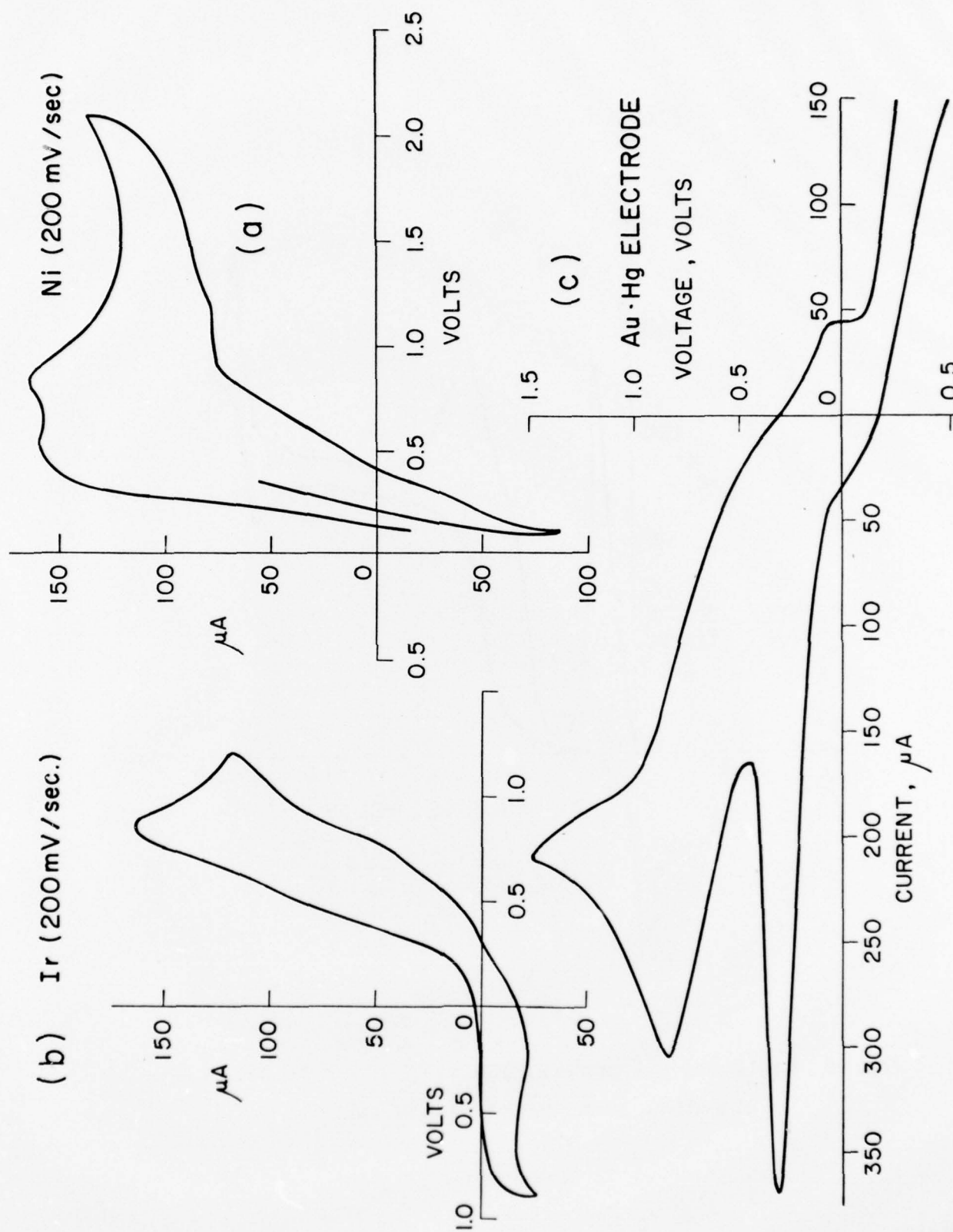


Fig. 25 Cyclic voltammograms of SOCl_2 in $\text{CH}_3\text{CN}/0.1\text{N N}(\text{C}_4\text{H}_9)_4 \text{PF}_6$ a) Ni wire electrode, b) Ir wire electrode, c) Au-Hg wire electrode ($V = .20\text{V/sec}$ in all)

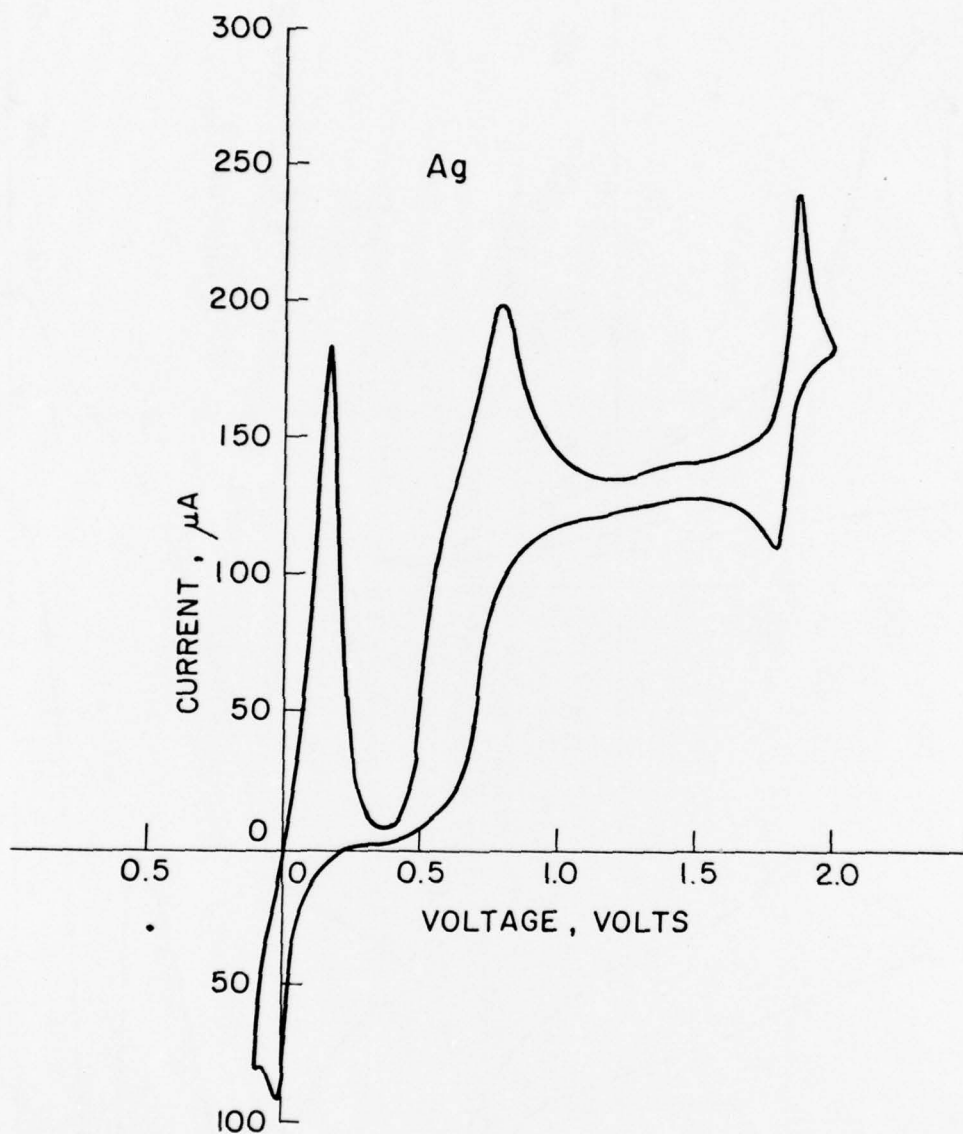


Fig. 26 Cyclic voltammogram of SCl_2 in $\text{CH}_3\text{CN}/0.1\text{N N}(\text{C}_4\text{H}_9)\text{PF}_6$
at a silver wire electrode (0.05V/sec)

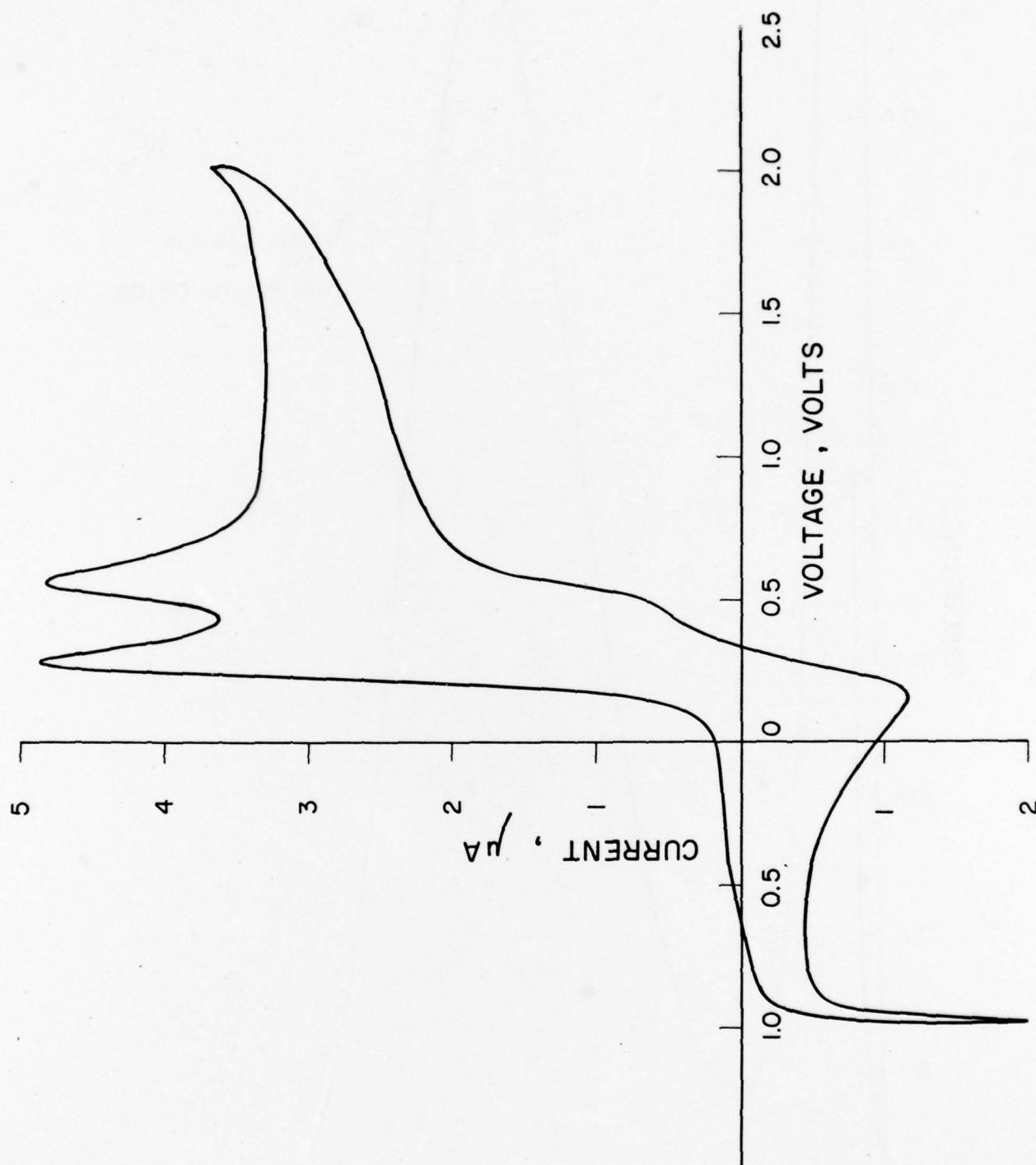


Fig. 27 Cyclic voltammogram of SCCl_2 in $\text{DMSC}/0.1\text{N } \text{N}(\text{C}_4\text{H}_9)_4 \text{PF}_6$ at a platinum wire electrode (0.05 V/sec)

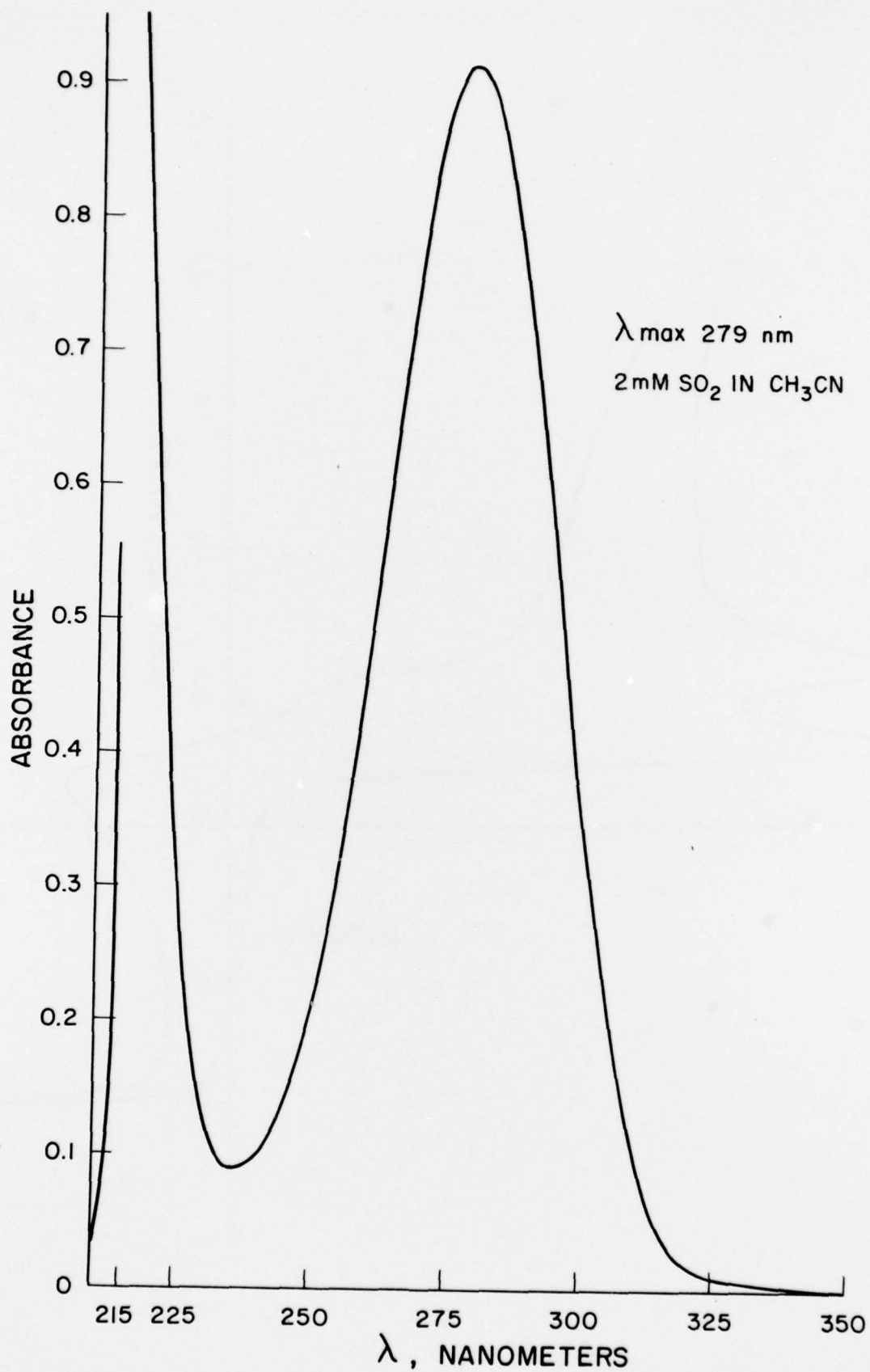


Fig. 28 UV-VIS spectrum of 2mM SO_2 in CH_3CN vs CH_3CN (pathlength 1 cm)

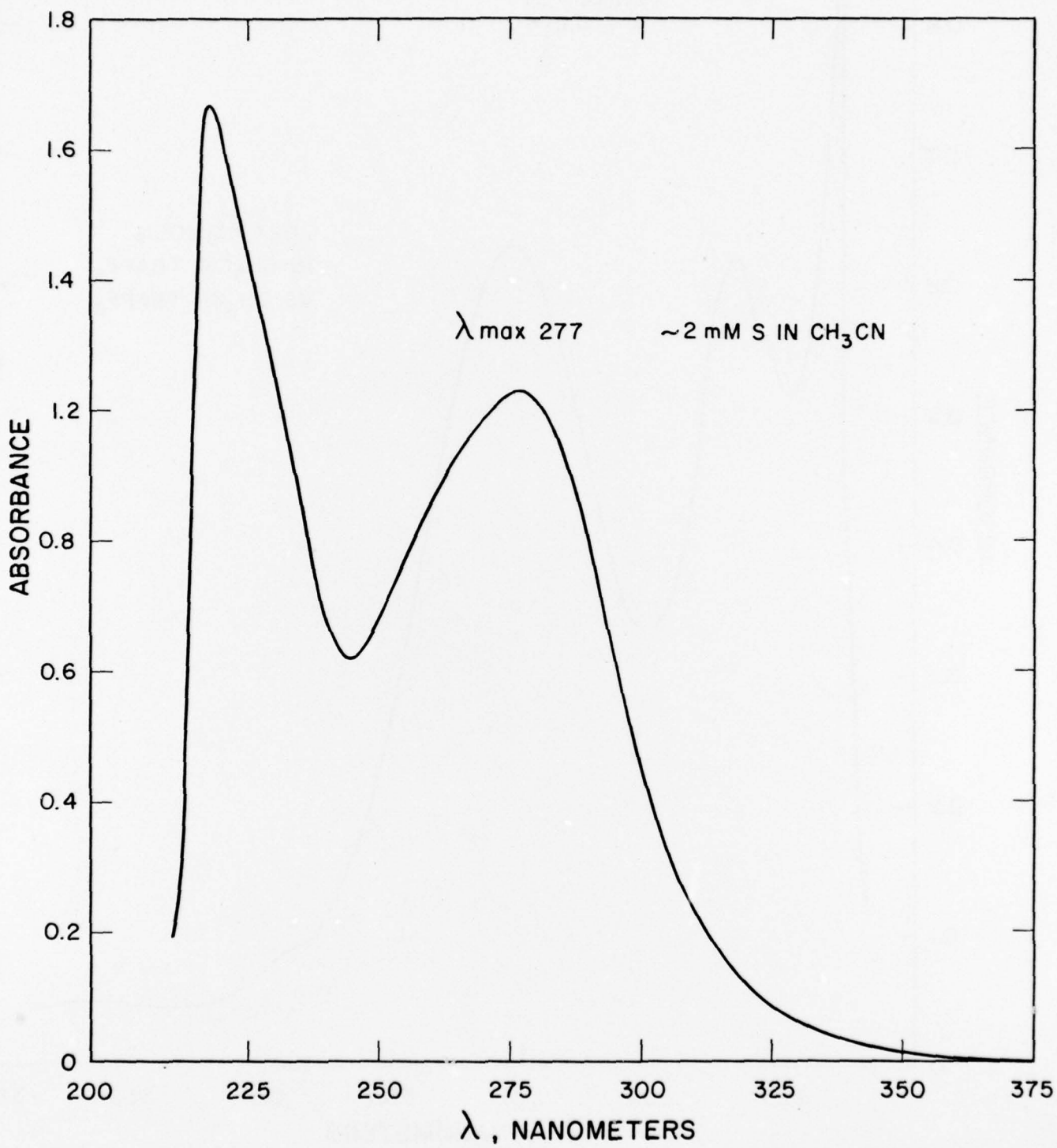


Fig. 29 UV-VIS spectrum of 2mM S in CH_3CN vs CH_3CN (pathlength 1 cm)

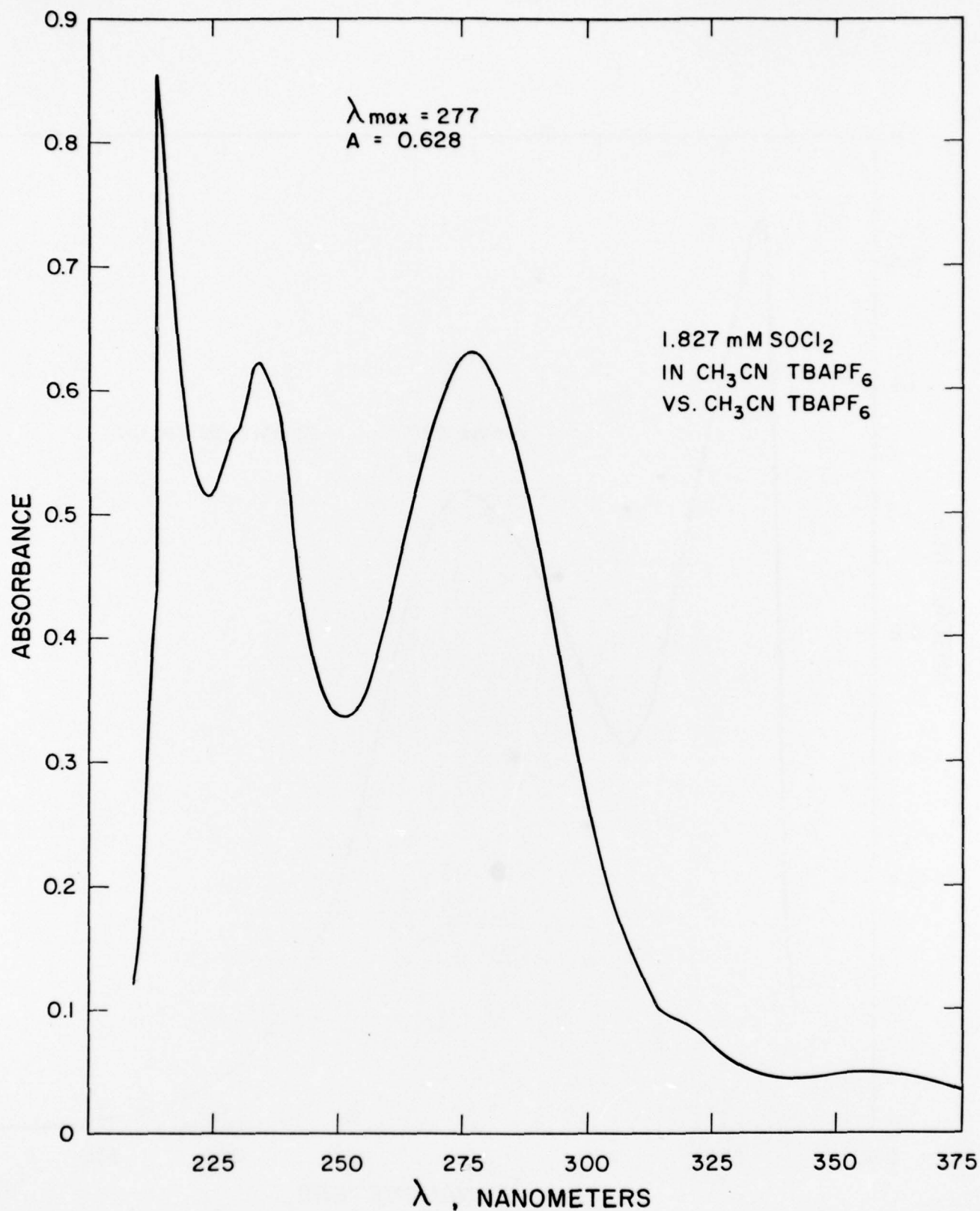
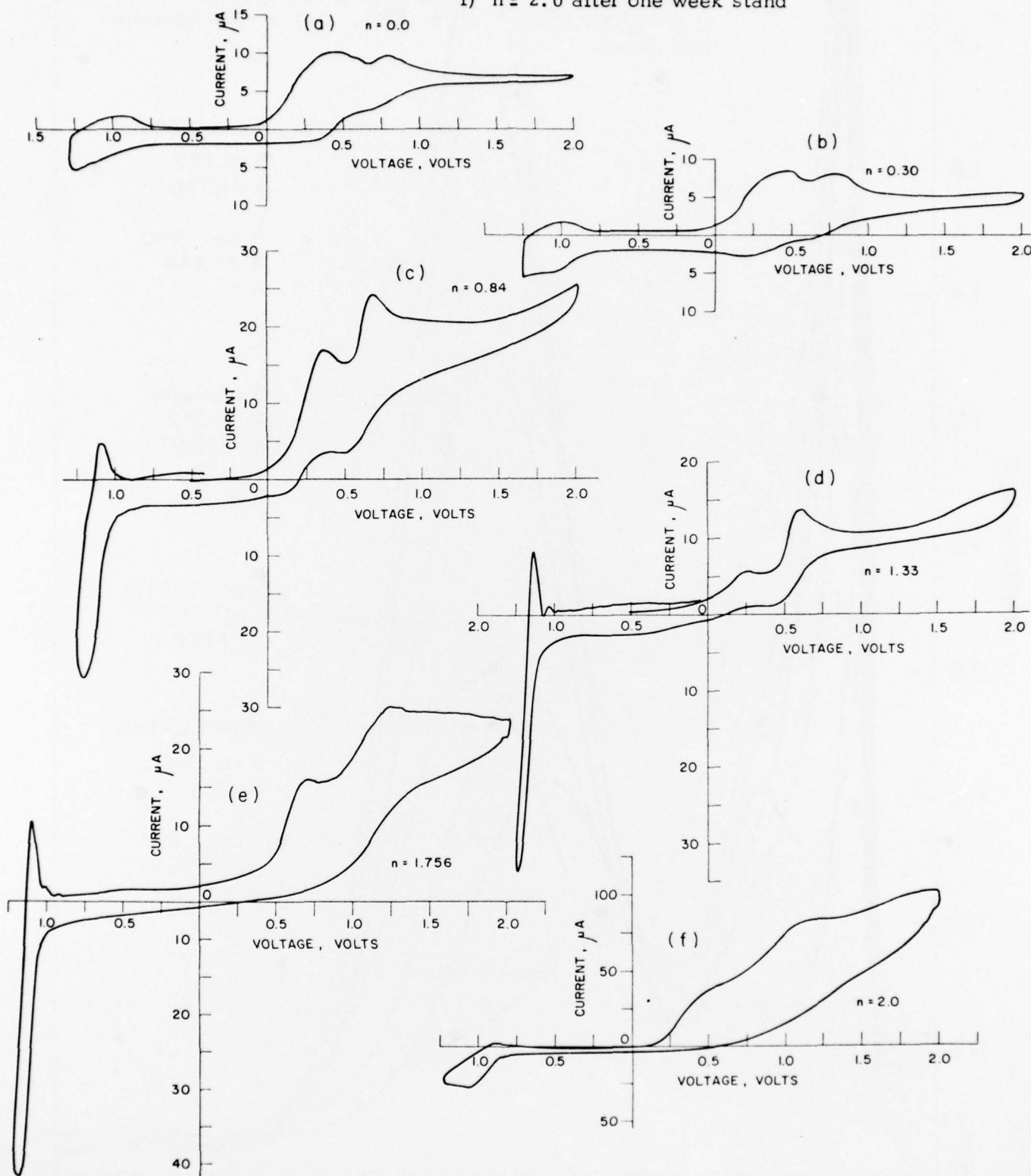
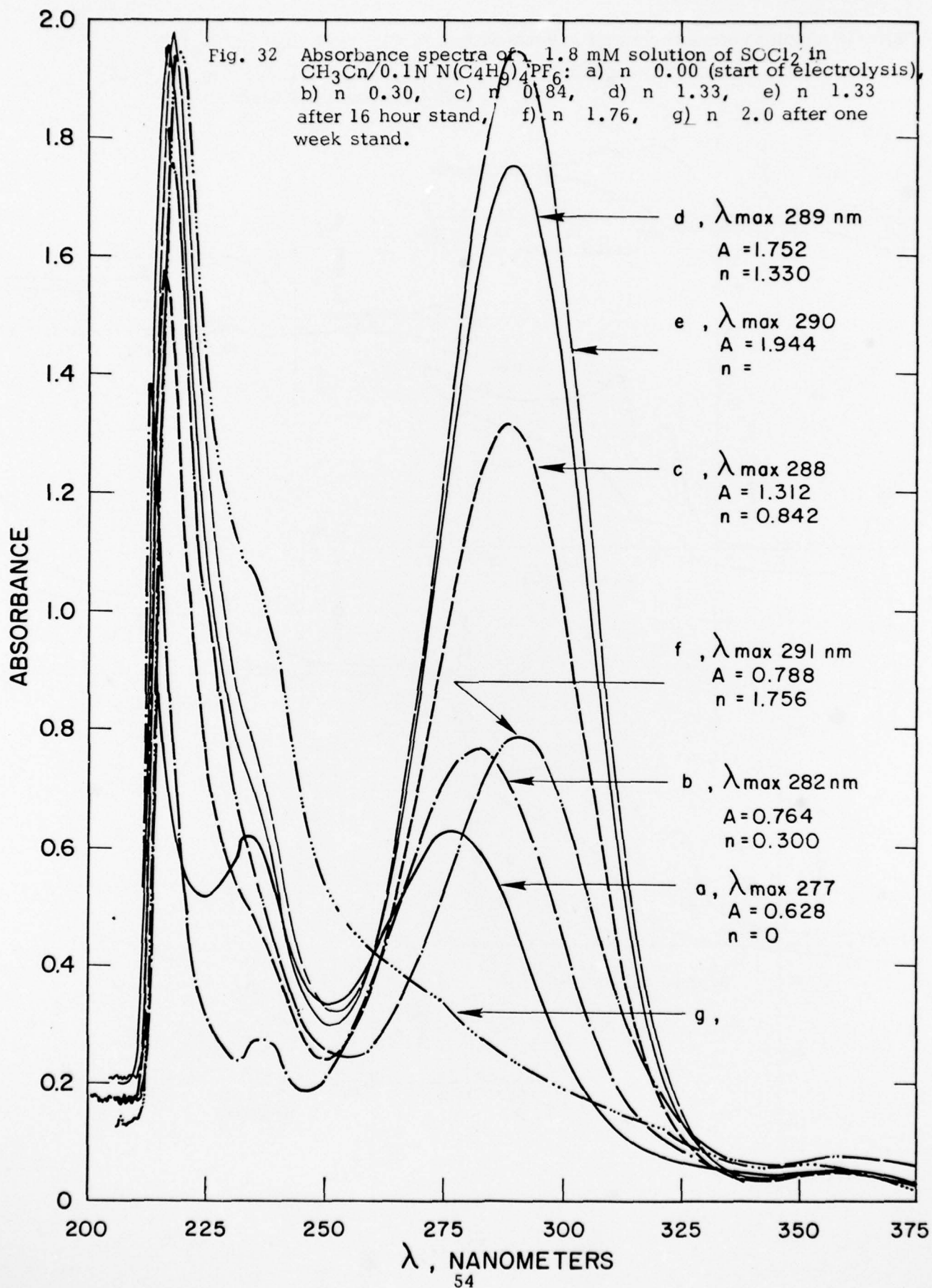


Fig. 30 UV-VIS spectrum of 1.8 mM SCl_2 in $\text{CH}_3\text{CN}/0.1\text{N N}(\text{C}_4\text{H}_9)_4\text{PF}_6$ vs $\text{CH}_3\text{CN}/0.1\text{N N}(\text{C}_4\text{H}_9)_4\text{PF}_6$ in a 1 cm pathlength cell

Fig. 31 Cyclic voltammogram of 1.8 mM SCl_2 in $\text{CH}_3\text{CN}/0.1\text{N N}(\text{C}_4\text{F}_9)_4\text{PF}_6$

a) $n = 0.00$, b) $n = 0.300$, c) $n = 0.84$, d) $n = 1.33$, e) $n = 1.76$,
f) $n = 2.0$ after one week stand





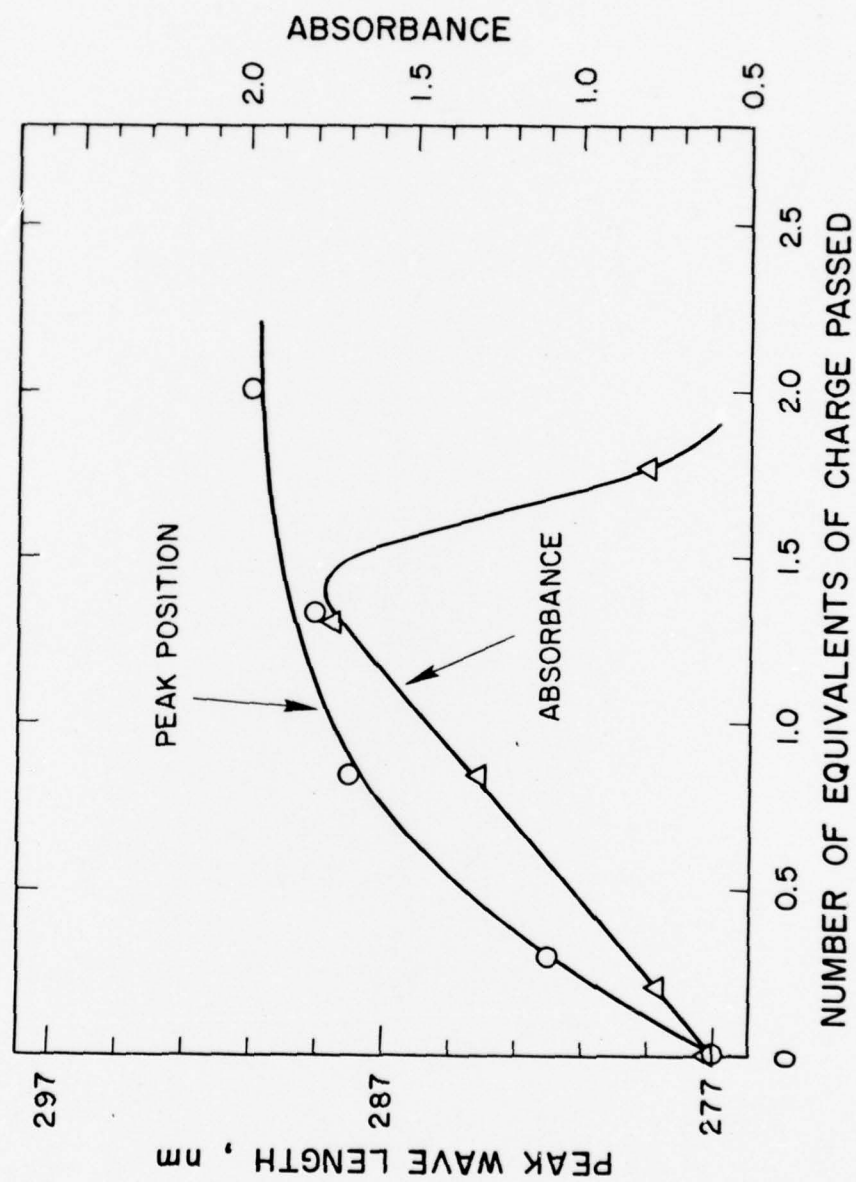


Fig. 33 Variation of λ_{max} and absorbance of SCl_2 solution as a function of charge passed during electrolysis

DISTRIBUTION LIST

Defense Documentation Center ATTN: DDC-TCA Cameron Station (Bldg 5) Alexandria, VA 22314	(12)	CDR, US Army Research Office ATTN: DRXRO-IP P.O. Box 12211 Research Triangle Park, NC 27709	(1)
Commander Naval Ocean Systems Center ATTN: Library San Diego, CA 92152	(1)	CDR, US Army Signals Warfare Lab ATTN: DELSW-OS Vint Hill Farms Station Warrenton, VA 22186	(1)
CDR, Naval Surface Weapons Center White Oak Laboratory ATTN: Library CODE WX-21 Silver Spring, MD 20910	(1)	Commander US Army Mobility Eqp Res & Dev CMD ATTN: DRDME-R Fort Belvoir, VA 22060	(1)
Commandant, Marine Corps HQ US Marine Corps ATTN: Code LMC Washington, DC 20380	(1)	Commander US Army Electronics R & D Command Forth Monmouth, NJ 07703	
Rome Air Development Center ATTN: Documents Library (TILD) Griffiss AFB, NY 13441	(1)	DELET-P DELET-DD DELET-DT DELS-D-L (TECH LIB) DELS-D-L-S (STINFO) DELET-PR	(1) (1) (2) (1) (2) (8)
Air Force Geophysics Lab/SULL ATTN: S-29 Hanscom AFB, MA 01731	(1)	Commander US Army Communications R & D Command Forth Monmouth, NJ 07703	
HQDA (DAMA-ARZ-D/DR. F.D. Verderame) Washington, DC 20310	(1)	USMC-LNO	(1)
CDR, Harry Diamond Laboratories ATTN: Library 2800 Powder Mill Road Adelphi, MD 20783	(1)	NASA Scientific & Tech Info Facility Baltimore/Washington Intl Airport PO Box 8757, MD 21240	(1)
Director US Army Materials Systems Analysis ACTV. ATTN: DRXSY-MP Aberdeen Proving Ground, MD 21005	(1)		

SUPPLEMENT TO DISTRIBUTION LIST

13 January 1978

Other Recipients

Mr. Donald Mortel (1)
AF Aero Propulsion Lab.
ATTN: AFAPL-POE-1
Wright-Patterson AFB, Ohio 45433

Mr. Richard E. Oderwald (1)
Department of the Navy
Hqs., US Marine Corps
Code LMC 4
Washington, DC 20380

Commander (1)
Harry Diamond Laboratories
ATTN: DELHD-RDD (Mr. A. Benderly)
2800 Powder Mill Road
Adelphi, MD 20783

Distribution List Continued

Transportation Systems Center Kendall Square Cambridge, MA 02142 ATTN: Dr. Norman Rosenberg	(1)	General Motors Corp. Research Laboratories General Motors Technical Center 12 Mile and Mounds Roads Warren, MI 48090 ATTN: Dr. J. L. Hartman	(1)
GTE Laboratories, Inc. 40 Sylvan Road Waltham, MA 02154	(1)	Union Carbide Corporation Parma Research Center P.O. Box 6116 Cleveland, OH 44101	(1)
Footo Mineral Company Route 100 Exton, PA 19341 ATTN: Dr. H. Grady	(1)	P. R. Mallory & Co., Inc. S. Broadway Tarrytown, NY 10591 ATTN: J. Dalfonso	(1)
Honeywell, Inc. 104 Rock Road Horsham, PA 19044 ATTN: C. Richard Walk	(1)	North American Roskwell Corp. Atomics International Division Box 309 Canoga Park, CA 91304 ATTN: Dr. L. Heredy	(1)
Sanders Associates, Inc. Sonobuoy Division 95 Canal Street Nashua, NH 03060 ATTN: Mr. David Dwyer	(1)	General Electric Research & Development Center P.O. Box 8 Schenectady, NY 12301 ATTN: D. Stefan Mitoff	(1)
Eagle-Picher Industries, Inc. Electronics Division ATTN: Mr. Robert L. Higgins P.O. Box 47 Joplin, Missouri 64801	(1)	University of California Department of Science & Research Santa Barbara, CA 93100 ATTN: Dr. J. Kennedy	(1)
Yardney Electric Company 82 Mechanic Street Pawcatuck, CT 02891 ATTN: Mr. William E. Ryder	(1)	The Electric Storage Battery Co. Carl F. Norburg Research Center 19 W. College Avenue Yardley, PA 19067 ATTN: Dr. A. Salkind	(1)
Exxon Research and Engineering Co. Corporate Research Laboratory Linden, NJ 07036 ATTN: Dr. R. Hamlen	(1)	Gulton Industries, Inc. Metuchen, NJ 08840 ATTN: Mr. S. Charlip	(1)
Argonne National Laboratories 9700 South Cass Argonne, IL 60439 ATTN: Dr. E. C. Gay	(1)	Electrochimica 2485 Charleston Road Mountain View, CA 94040 ATTN: Dr. Eisenberg	(1)
GTE Sylvania, Inc. 77A Street Needham Heights, MA 02194 ATTN: Mr. Richard Pabst	(1)		

Distribution List Continued

Dr. Hugh Barger P.O. Box 2232 Davidson, NC 20836	(1)	NASA Lewis Research Center Mail Stop 6-1 21000 Brookpark Road Cleveland, OH 44135 ATTN: Dr. Stuart Fordyce	(1)
Energy Storage & Conversion Dept. TRW Systems One Space Park Redondo Beach, CA 90278 ATTN: Dr. H.P. Silverman	(1)	Mr. Joe McCartney Naval Undersea Center Code 608 San Diego, CA 92132	(1)
Sanders Associates, Inc. 24 Simon Street Mail Stop NSI-2209 Nashua, NH 03060 ATTN: J. Marshall	(1)	EIC, Inc. ATTN: S. B. Brummer Newton, MA 02158	(1)
Power Conversion, Inc. 70 MacQuesten Pkwy Mount Vernon, NY 10550 ATTN: Stuart Chodosh	(1)	Altus Corp. 440 Page Mill Road Palo Alto, CA 94306 ATTN: Douglas Glader	(1)
Dr. D. Pouli Portfolio Manager Hooker Chemicals & Plastics Corp. M.P.O. Box 8 Niagara Falls, NY 14302	(1)	J. Bene MS 488 NASA Langley Research Center Hampton, VA 23665	(1)
Dr. Leonard Nanis G207 S.R.I. Menlo Park, CA 94025	(1)	Mr. Eddie T. Seo Research and Development Div. The Gates Rubber Co. 999 S. Broadway Denver, CO 80217	(1)
Dr. J. J. Auburn, RM 1A-317 Bell Laboratories 600 Mountain Avenue Murray Hill, NJ 07974	(1)	Mr. Sidney Gross Mail Stop 8C-62 Boeing Aerospace Company P.C. Box 3999 Seattle, WA 98124	(1)
Stonehart Associates, Inc. 34 Five Fields Road Madison, CT 06443 ATTN: Mr. Thomas Reddy	(1)	Honeywell Technology Center ATTN: Dr. H.V. Venkatesetty 10701 Lyndale Avenue South Bloomington, MN 55420	(1)
Mr. J. R. Moden Energy Conversion Branch Code 3642 Naval Underwater Systems Center Newport Laboratory Newport, RI 02840	(1)		

79

